



Sveriges
lantbruksuniversitet

Modeling of bark-, sand- and activated carbon filters for treatment of greywater

Susanna Ciuk Karlsson

George Edward Pelham Box:

“Essentially, all models are wrong, but some are useful.”

ABSTRACT

Modeling of bark-, sand- and activated carbon filters for treatment of greywater

Susanna Ciuk Karlsson

The part of the waste water produced in a household, originating from showers, dish - and wash water, is called greywater. It is possible to treat the greywater separately from the black water (toilet water) as it is less polluted and then use it for purposes such as garden irrigation. There are various methods for purifying greywater. Here, the possibility to purify greywater using three column filters with different materials (activated carbon, pine bark and sand) was examined through modeling in the computer program HYDRUS.

A set-up with physical filters was available, where flow measurements were performed. These measurements were used to validate the model that was developed in HYDRUS. When a flow model had been produced that could replicate the measured flow, a module of HYDRUS was used to also model the reactive transport of nutrients and organic matter in the filters.

The complete model was used for evaluation of the treatment performance of the filters during a default scenario where they were loaded with 1 liter of water per day containing pollutant concentration corresponding to typical greywater.

Keywords: Wastewater reuse, modeling, filters, organic matter, nutrients
Department of Energy and Technology, Swedish University of Agricultural Sciences
Lennart Hjelms väg 9
SE-750 07 Uppsala, Sweden

REFERAT

Modellering av bark-, sand- och kolfilter för rening av BDT-vatten

Susanna Ciuk Karlsson

I ett hushåll används vatten som då blir till avloppsvatten. Detta avloppsvatten består till stor del av bad, disk och tvättvatten (BDT-vatten). Det är möjligt att behandla BDT-vattnet separat från klosettvattnet då det är mindre förorenat, låta det genomgå rening och sedan använda det för till exempel bevattning av trädgårdar. Det finns olika metoder för att rena BDT-vatten. Här studerades möjligheterna att rena BDT-vatten med hjälp av tre filter av olika material; aktivt kol, tallbark och sand, genom modellering i datorprogrammet HYDRUS.

En praktisk experimentuppsättning med filterkolonner fanns att tillgå, där ett experiment med flödesmätningar genomfördes. Mätningarna användes för att validera modellen som utvecklades i HYDRUS. Efter att en flödesmodell som stämde överrens med uppmätta värden utvecklats, modellerades reaktiv transport av näringsämnen och organiskt material i filtren med en modul tillhörandes HYDRUS.

Med hjälp av modelleringen kunde filtertypernas reningsförmåga utvärderas för ett iscensatt standardscenario där filtrena belastades med 1 l vatten/dag innehållandes föroreningar motsvarandes ett typiskt gråvatten.

Nyckelord: Avloppsvatten, modellering, filter, organiskt material, näringsämnen
Institutionen för energi och teknik, Sveriges Lantbruksuniversitet, Lennart Hjelm's väg 9
SE-750 07 Uppsala, Sverige

PREFACE

This is the master thesis which finalizes my Master's degree in Environmental and Water Engineering at Uppsala University. The master thesis is for 30 ECTS credits and was carried out at the Swedish University of Agricultural Sciences. Supervisors of this project were Sahar Dalahmeh and Cecilia Lalander, with subject reviewer Håkan Jönsson, all active at the Department of Energy and Technology.

The master thesis is a part of a research project which aims at developing and applying filters individually made of pine bark, activated charcoal and sand material for on-site greywater treatment so that the purified greywater can be reused as a resource for irrigation, service or recharge of surface-and groundwater. This research project is financed by Swedish International Development Cooperation Agency, Sida and by the Swedish Research Council Formas.

I sincerely thank all who became involved in the making of this thesis. I thank my supervisors Sahar Dalahmeh and Cecilia Lalander. Also, thanks to my cheerful subject reviewer Håkan Jönsson. Special thanks to Sven Smårs who happily and frequently aided with the practical set-up and Gunther Langergraber, who gave a modeling crash course which was absolutely vital to the success of the thesis. At last, great thanks to Allan Rodhe who can be truly admired for his efforts as examiner.

Anecdotal information: A humongous amount of coffee was consumed during the making of this master thesis.

Uppsala, 2012

Susanna Ciuk Karlsson

Copyright© Susanna Ciuk Karlsson and Department of Energy and Technology,
Swedish University of Agriculture
UPTEC W 12029, ISSN 1401-5765
Printed at the Department of Earth Sciences, Geotryckeriet, Uppsala University,
Uppsala, 2012.

POPULÄRVETENSKAPLIG SAMMANFATTNING

Modellering av bark-, sand, och kolfilter för rening av BDT-vatten

Susanna Ciuk Karlsson

Hushåll överallt i världen har åtminstone en sak gemensamt: det dagliga behovet av vatten. När vatten har använts i ett hushåll kommer det att vara förorenat. Avfallsvattnet består till en del av bad, disk och tvättvatten (BDT-vatten). BDT-vattnet innehåller kemikalier från tvättmedel, kroppsvårdsprodukter, en viss mängd bakterier och organiskt material från kök. Sammansättningen varierar från hushåll till hushåll och beroende på tillgången på vatten kommer koncentrationerna att variera. Ungefär två tredjedelar av vattnet som lämnar hushållet är BDT-vatten. Det är möjligt att behandla BDT-vattnet separat från klosettvattnet (vatten från toaletten), låta det genomgå rening och sedan gå till användning för till exempel bevattning av trädgårdar. Återanvändning av BDT-vatten är särskilt viktigt för hushåll med begränsad tillgång till vatten.

Det finns olika metoder för att rena BDT-vatten. Här studerades möjligheterna att rena BDT-vatten med hjälp av tre filter bestående av olika material; aktivt kol, tallbark och sand. Sand har använts sedan länge som material i markbäddar och anlagda våtmarker medan bark och kol är relativt outforskade material att använda i filter. Både bark och kol har betydligt lägre densitet än sand, vilket underlättar transport av materialen. Båda kommer som restprodukter ur industri och kan därför förmodas finnas tillgängliga till lågt pris. Filtrena studerades genom modellering i programvaran HYDRUS. HYDRUS modellerar specifikt flödesdynamik och ämnestransport genom naturjordar.

En experimentuppställning för att testa materialen fanns tillgänglig, bestående av sex kolonner. De var 1 meter höga, hade en radie på 10 cm och var fyllda med materialen upp till 60 cm. Två kolonner var fyllda med bark, två med kol och två med sand. Experimentuppställningen användes för flödesmätningar. Filtrena matades ovanifrån med kranvatten, totalt en liter per dag uppdelat i tre mängder: 0,7 L, 0,1 L och 0,2 L vid klockan 9.00, 16.00 och 20.00, respektive. Matningen skedde automatiskt via dator. Vattnet rann genom filtret och passerade ut genom en slang till en hink. Hinken var uppställd på en våg kopplad till en dator och ett värde på vikten dokumenterades varje minut. På så sätt samlades mätningar av det kumulativa flödet genom filtret. Även mätningar med dubblerat flöde genomfördes.

Mätningarna användes för att validera flödesmodellen som framarbetades i HYDRUS. Efter att en realistisk flödesmodell sammanställts användes en modul till HYDRUS, CW2D, för att även modellera reaktiv transport av näringsämnen och organiskt material i filtrena. CW2D är skapad som ett tillägg till HYDRUS för att särskilt studera anlagda våtmarker. CW2D beskriver sammanlagt nio processer och tolv komponenter som verkar i en anlagd våtmark. Samma processer och komponenter kunde anses vara verksamma även i filtertypen som användes i denna undersökning. Processerna som studerades var nitrifikation, denitrifikation, hydrolys och tillväxt och avdödning av mikroorganismer. Det var dessa processer som ansågs utgöra reningsmekanismen inuti

filtret. I processerna var många komponenter inblandade och de studerades, speciellt omvandlingen emellan dem och ämnens transport genom filtret (reaktiv transport). Organiskt material beskrevs i tre former, lättillgängligt COD, svårtillgängligt COD och inert COD. COD är ett mått som beskriver mängden förbrukat syre vid fullständig kemisk nedbrytning av organiska ämnen i vatten. Fyra former av kväve studerades: nitrat, nitrit ammonium och kvävgas. Även oorganisk fosfor studerades, samt bildandet av biomassa bestående av mikroorganismer. Mikroorganismerna var i CW2D uppdelade i tre kategorier: heterotrofa mikroorganismer, Nitrosomonas och Nitrobacter, varav de två sistnämnda är autotrofa mikroorganismer.

Modellen byggdes upp så att den simulerade att filtret utsattes för en standardbelastning. Standardbelastningen var bestämd utifrån uppskattningen av hur vattenförbrukningen i ett hushåll ser ut. Från en hydrograf bestämdes mängden vatten och vid vilka tidpunkter vattenmängden skulle tillföras filtret. Föroreningarna i vattnet skulle motsvara ett typiskt gråvatten. Simuleringen fick fortgå i 113 dagar och den långa simuleringstiden gjorde det möjligt att studera hur det simulerade utgående vattnet skulle ändra karaktär med tiden. En modell för varje filtertyp framställdes, så att filtermaterialens olika egenskaper kunde simuleras specifikt.

De framställda modellerna kunde generera flödessimuleringar som stämde väl överrens med uppmätta värden av det kumulativa flödet för samtliga filtertyper. Intressanta simuleringar för framtiden skulle vara att modellera större filter med ett flöde i samma skala som det som kommer från ett hushåll.

Till stöd för modelleringen av den reaktiva transporten fanns mätningar tillgängliga från ett föregående experiment. Då hade samma experimentuppställning använts men istället för att mata filtrena med kranvatten hade ett konstgjort BDT-vatten framställts. Mätningar av halter organiskt material, kväve och fosfor gjordes sedan på det utgående vattnet från filtrena. Modellen var uppbyggd så att det simulerade ingående vattnet motsvarade det framställda BDT-vattnet.

Simuleringsresultatet för sandfiltret visade sig stämma bra överrens med uppmätta värden för reduktion av COD och fosfor. Modellen fångade även upp att organiskt kväve omvandlades till stor del till nitrat. Det var svårare att se en överensstämmelse mellan simuleringarna och mätningarna för de andra filtertyperna, bark och kol. Det är möjligt att förmodade absorptionsegenskaper hos kol- och barkmaterialen inte kunde beskrivas med programvaran HYDRUS som främst riktar in sig på olika typer av naturjord.

GLOSSARY

BARK1, BARK2, CHAR1, CHAR2, SAND1, SAND2: Naming of the filters, corresponding to the different filter materials used: bark, activated carbon and sand. Each filter type had a duplicate, resulting in 6 filters total.

BOD₅: Amount of oxygen consumed by biochemical oxidation of waste contaminants in a 5-day period

BOD_u: Amount of oxygen consumed by biochemical oxidation of waste contaminants in a 28-day period

COD: Chemical oxygen demand

CI: Inert soluble COD

CR: Readily biodegradable soluble COD

CS: Slowly biodegradable soluble COD

CW: Constructed wetland

DW: Dry weight of filter media

HE: Heterotrophic microorganisms

IP: Inorganic phosphorus

N₂: Dinitrogen gas, N₂

NB: Nitrobacter

NH₄N: Ammonium, NH₄⁺ and ammonia, NH₃

NO₂N: Nitrite, NO₂⁻

NO₃N: Nitrate, NO₃⁻

NS: Nitrosomonas

TN: Total nitrogen

TP: Total phosphorus

TABLE OF CONTENTS

ABSTRACT	II
PREFACE.....	IV
POPULÄRVETENSKAPLIG SAMMANFATTNING	V
GLOSSARY	VII
1. INTRODUCTION	1
1.1 BACKGROUND: GREYWATER.....	1
1.2 ASSOCIATED RESEARCH PROJECT.....	1
1.2.1 Vertical flow filters.....	2
1.3 BACKGROUND: MODELLING	3
1.4 OBJECTIVE	4
2. THEORY	5
2.1 HYDRUS AND THE CONSTRUCTED WETLAND MODULE.....	5
2.1.1 Richard's equation.....	5
2.1.2 van Genuchten approach	6
2.2 SOLUTE TRANSPORT	6
2.3 COMPONENTS AND PROCESSES.....	7
2.4 APPLIED NUMERICAL METHODS OF HYDRUS	8
3. METHOD	9
3.1 MATERIAL.....	9
3.2 DATA COLLECTION	10
3.2.1 Sprinkler investigation.....	11
3.3 HYDRUS MODEL BUILDING	11
3.3.1 Simulating water flow through the filters using HYDRUS.....	11
3.3.2 Calibrating the model by tuning empirical coefficients	13
3.4 REACTIVE TRANSPORT MODELING	13
4. RESULT PART I: FLOW EXPERIMENTS AND SIMULATION	16
4.1 SPRINKLER INVESTIGATION.....	16
4.2 RESULTS: EMPIRICAL EXPERIMENT	16
4.2.1 Bark filter.....	16
4.2.2 Charcoal filter	18
4.2.3 Sand filter	19
4.2.4 Comparison between filters	21

4.3 CALIBRATION RESULTS	21
4.4 SIMULATED FLOWS.....	22
4.4.1 Bark filter.....	22
4.4.2 Charcoal filter.....	23
4.4.3 Sand filter	24
4.4.4 Validating estimated empirical coefficients	24
5. RESULT PART II: REACTIVE TRANSPORT SIMULATIONS.....	26
5.1 BIOMASS FORMATION.....	26
5.2 ORGANIC MATTER DEGRADATION	27
5.2.1 Readily biodegradable soluble COD	27
5.2.2 Slowly biodegradable soluble COD	28
5.2.3 Inert soluble COD.....	28
5.3 INORGANIC PHOSPHORUS CONCENTRATION.....	30
5.4 NITROGEN TRANSFORMATION	32
5.4.1 Nitrate concentration	32
5.4.2 Ammonium and ammonia concentration	34
5.4.3 Nitrite concentration.....	35
5.4.4 Dinitrogen concentration	36
5.5 SUMMARIZED RESULTS FOR THE REACTIVE TRANSPORT MODELING	37
6. DISCUSSION.....	39
6.1 FLOW DYNAMICS.....	39
6.2 MODELING OF BIOMASS	40
6.3 MODELING OF ORGANIC MATTER DEGRADATION	40
6.4 MODELING OF NUTRIENT TRANSFORMATION.....	41
6.4.1 Phosphorus	41
6.4.2 Nitrogen.....	42
6.5 MODELING AS A TOOL TO EVALUATE DESIGN CRITERIA.....	43
6.6 RECENT RESEARH ASSOCIATED TO CW2D	43
6.7 GENERAL REMARKS	44
7. REFERENCES	46

1. INTRODUCTION

At present 2.4 billion people do not have access to proper sanitation services (Langergraber and Muellegger, 2004). In the parts of the world which is the poorest and where scarcity of water is severe, for example in India, less than 50 % of the urban population has access to sewage disposal systems. Their wastewater, which contains pathogens and toxic chemicals, is disposed directly into water bodies. When the contaminated water bodies are used as resources to irrigate farm land, the toxic chemicals will pass on to plants and into the food chain and ultimately affect public health. Even more unsettling, about 60 % of deaths in the urban population can be traced to lack of access to safe drinking water facilities (Aktar, 2007). The situation urgently calls for a sustainable solution to treat wastewater, so that it can be reused to cover a most pressing need for water and also to prevent further pollution of natural water bodies.

1.1 BACKGROUND: GREYWATER

Domestic wastewater is composed of toilet water (also called blackwater) and water from other sources such as kitchen services, laundry and washing facilities (greywater) (Muellegger et al., 2003).

About one third of the domestic wastewater consists of black-water and the other two thirds of greywater. Greywater compared to black-water, contains less nutrients. In comparison, typical municipal wastewater has a BOD₅:N:P ratio of 100:20:5 while greywater has a ratio of 100:4:1 (Muellegger et al., 2003). The concentrations for phosphorus, heavy metals and xenobiotic organic pollutants are about the same (even though one must bear in mind that the constitution of the greywater depends heavily on the household producing the waste, making general conclusions on greywater characteristics uncertain).

Fecal contamination of greywater occurs from situations which include diaper laundry, childcare, anal cleansing and showering. The fecal contamination of greywater in Sweden is 980 times lower than in typical municipal wastewater. Greywater has plenty of easily degradable organic compounds. Enteric bacteria which are used as fecal indicators might grow because of this, which will be misleading for determining the amount of pathogens (Ottoson, 2005).

Since greywater and blackwater are so different, separation of the two becomes interesting. If greywater and blackwater is separated, the treatment and usage can be adapted to the different characteristics. One expected result of the adaption is lowered energy costs due to increased efficiency (Muellegger et al., 2003).

1.2 ASSOCIATED RESEARCH PROJECT

This master thesis is associated to the research projects, “On-site treatment of greywater – upgrading to a resource for irrigation, service or recharge” and “On-site treatment of greywater – production of a water resource”, which both aims to develop and apply

filters made of pine bark, activated carbon and sand material for on-site greywater treatment, so that the treated greywater can be reused as a resource for irrigation, service or recharge of surface-and groundwater. These research projects are financed by Swedish International Development Cooperation Agency, SIDA and the Swedish Research Council Formas, respectively.

The specific objectives are to investigate different organic filter materials, develop design criteria for vertical filters and to design and construct pilot facilities in Uganda, Ghana and Jordan. Also as a specific objective is to initially evaluate the three pilot facilities and disseminate the results.

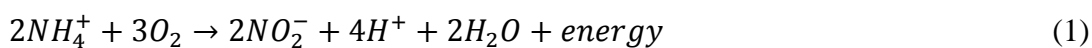
These research projects were carried out by the Department of Energy and Technology at Swedish University of Agricultural Sciences and were expected to run for 3 years, finishing in the end of 2013 and end of 2015, respectively.

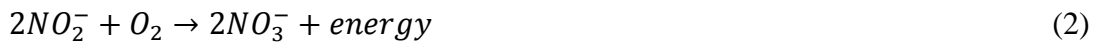
1.2.1 Vertical flow filters

The filters used in this study were rather similar to vertical flow constructed wetlands (VF CW) although with some differences. Both are column like constructions, which are fed intermittently with wastewater at the top. The wastewater is pulled down through the porous media by gravity (Haberl et al., 2003). The difference is mainly that the vertical flow filter is not planted and natural soil is not used as filter material. The sand filter is more similar to a VF CW than the bark and charcoal filters, since sand is used in many VF CW. The sand filter serves a purpose as a reference when evaluating the treatment outcome of the filters. Bark and charcoal are regarded as interesting replacement material of sand, since sand is a heavy material which is difficult to transport. Bark and charcoal on the other hand are light weight and can in some locations be a cheaper alternative than sand since both bark and charcoal might be available as residual waste. Also, the bark and charcoal as filter materials could possibly provide better treatment properties than sand due to their large specific areas which promotes adsorption and biofilm development (Dalahmeh et al., 2012).

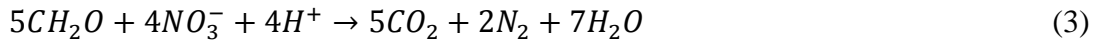
As in the case of a VF CW, after a loading the greywater will drain vertically through the filter material by force of gravitation. The water will not completely saturate the filter material, meaning the flow will be transient variable saturated. That is, the pores of the filter material will intermittently contain water and air and this makes the matter of flow less predictable than in the case of a completely saturated porous material where all the pores are water filled. In between the loadings, which are intermittent, air will reenter most of the pores of the filter material. This aeration provides oxygen which creates an aerobic environment within the filter, hence allowing for aerobic processes such as degradation of organic matter and nitrification to occur (Langergraber and Simunek, 2005).

Nitrification is a two-step process (Eriksson et al., 2005):





The first step is often performed by Nitrosomonas and the second step by Nitrobacter, two types of autotrophic bacteria. Denitrification on the other hand, is an anoxic process including heterotrophic bacteria (HE) (Eriksson et al., 2005):



The denitrification inside the filter is one of many mechanisms involved within the filter. Central to the treatment is the presence of microorganisms and the degradation process of organic material (Figure 1).

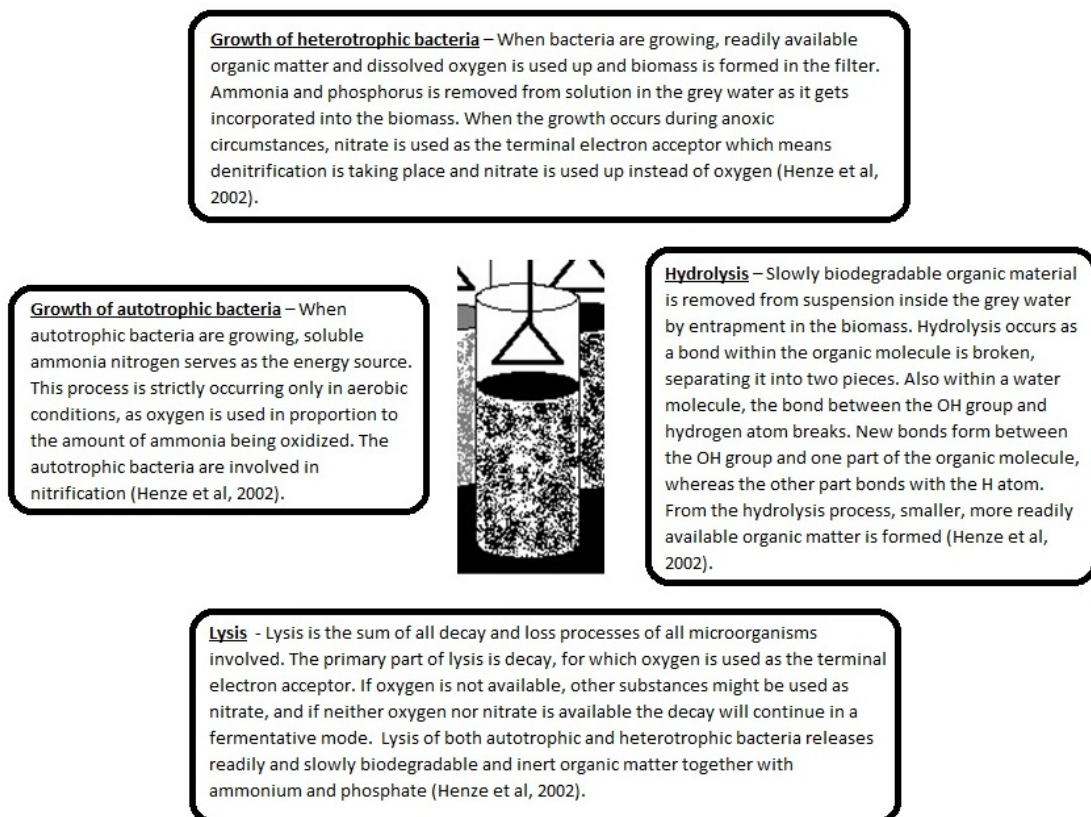


Figure 1 Descriptive diagram explaining some processes involved in treatment of greywater within a filter, displaying a set-up of a filter with sprinkler in the middle.

1.3 BACKGROUND: MODELLING

Since the filters are similar to a VF CW, models existing for constructed wetlands (CW) can be an interesting tool in assessing the performance of the filters.

From a modeling perspective the process within a CW has long been regarded as a black box (Langergraber, 2011). Although a CW is simple to build and use, the inside mechanism is highly versatile including chemical, biological and physical processes that all occur in parallel, affecting each other. Rather than understanding the underlying processes governing the treatment, CW has so far been considered as treatment systems with incoming wastewater and outgoing treated effluent. The dimensioning has thus

been based on rule of thumb approaches with rough estimations of specific surface areas required (Langergraber, 2011).

With enhanced computer capacity and advanced numerical methods, the quest to develop adequate computer models describing the processes occurring in the CW have been undertaken by different researchers. There are models ranging from simple transport and first-order decay models to complex mechanistic models. The best known of the simpler models are: the method of moments; the dispersed plug-flow; the tanks in series; and the detention time gamma distribution. The simpler models are easy to use but the results will be rather blunt since the underlying assumptions are leaving out important information such as temperature dependencies (Langergraber et al., 2008). Belonging to the more complex models is CW2D, a multi-component reactive transport module created for the water flow and transport modeling software HYDRUS. Complex mechanistic models describe transformation and decay processes in detail but are difficult to use because of their complexity (Langergraber et al., 2008).

1.4 OBJECTIVE

The main objective of this master thesis was to model water flow dynamics, organic matter degradation and nutrient transformation of greywater filtrated through bark, charcoal and sand filters using the wetland module for HYDRUS. The simulated results of the model were compared to empirical data measured from a practical experiment.

The overall aim of the modeling task was to better understand the processes governing the greywater treatment performance of these vertical flow filters and compare the results of the three different materials.

2. THEORY

2.1 HYDRUS AND THE CONSTRUCTED WETLAND MODULE

HYDRUS is a Microsoft Windows based modeling tool for analyzing water flow and solute transport in variably saturated porous media. The constructed wetland module of HYDRUS comes in two different versions, CW2D and CWM1. These are both multicomponent reactive transport modules that describe the biochemical transformation and degradation processes for organic matter, nitrogen and phosphorus in CW. CW2D and CWM1 are based on the same principles used for the activated sludge models (ASM) that were developed by the International Water Association (Langergraber, 2011). Here CW2D was used because of its capacity to handle transient variable-saturated flow. CW2D also provides modeling of nitrification as a two-step process, which appeals to the objective of this thesis.

2.1.1 Richard's equation

The governing equation of water flow in HYDRUS is a modified form of Richard's equation, a partial differential equation covering two- and/or three-dimensional isothermal uniform Darcian flow of water in a variably saturated rigid porous medium. It is valid under assumption that the air phase plays an insignificant role in the liquid flow process and it is stated (Simunek et al., 2006):

$$\frac{\partial \theta}{\partial t} = \frac{\partial}{\partial x_i} \left[K \left(K_{ij}^A \frac{\partial h}{\partial x_j} + K_{iz}^A \right) \right] - S \quad (4)^*$$

where symbol notation are as follows:

- L: length unit after preference;
- T: time unit after preference;
- θ : volumetric water content, [L^3/L^3];
- h : pressure head, [L];
- S : sink term, [T^{-1}];
- x_i : spatial coordinates ($i = 1,2$), [L];
- t : time [T];
- K_{ij}^A : components of a dimensionless anisotropy tensor \mathbf{K}^A . This is used to account for an anisotropic medium (the diagonal entries of K_{ij}^A equals one and the off-diagonal entries zero if the medium is isotropic);
- K : unsaturated hydraulic conductivity function, [L/T].

The conductivity of water in an unsaturated system is given by:

$$K(h, x, y, z) = K_s(x, y, z)K_r(h, x, y, z) \quad (5)$$

with K_r as relative hydraulic conductivity and K_s the saturated hydraulic conductivity [L/T].

* Einstein summation convention used

2.1.2 van Genuchten approach

The unsaturated hydraulic conductivity and the soil water retention behave in general as nonlinear functions of the pressure head. HYDRUS provides five different analytical models for the hydraulic properties. In this work the van Genuchten approach (Simunek, J. and van Genuchten, M.Th. and Sejna, M., 2006) was used, due to its status as being most commonly used:

$$\theta(h) = \begin{cases} \theta_r + \frac{\theta_s - \theta_r}{[1 + |\alpha h|^n]^m} & h < 0 \\ \theta_s & h \geq 0 \end{cases} \quad (6)$$

$$K(h) = K_s S_e^l \left[1 - (1 - S_e^{1/m})^m \right]^2 \quad (7)$$

$$m = 1 - \frac{1}{n} \quad n > 1 \quad (8)$$

With:

- θ_r, θ_s : residual and saturated water content [L^3/L^3];
- K_s : saturated hydraulic conductivity [L/T];
- α : inverse of the air-entry value, or bubbling pressure [L^{-1}];
- n : a pore-size distribution index [-];
- l : a pore-connectivity parameter [-].

The parameters l , n and α impacts upon the shape of the hydraulic functions and can be treated as empirical coefficients. For l , the value 0.5 can be used as it is an estimated average for many soil types.

The other four methods which are implemented in HYDRUS, that can be freely chosen for computations, are: Brooks and Corey (1964); Vogel and Cislerva (1988); Kosugi (1995); and Durner (1994).

The description of the variably saturated water flow in HYDRUS also includes root water uptake and dual porosity systems. HYDRUS takes into account the temperature dependence of the soil hydraulic functions based on capillary theory that assumes that the effect of temperature on capillary pressure is a linearly decreasing function of temperature. In many flow simulations the simplification can be used that hysteresis does not need to be taken into consideration for the soil hydraulic properties. However, if a more realistic description is required, HYDRUS provides tools to include hysteresis as well (Simunek, J. and van Genuchten, M.Th. and Sejna, M., 2006).

2.2 SOLUTE TRANSPORT

For the macroscopic transport of components in the system, denoted i , the following equation is used:

$$\frac{\partial \theta c_i}{\partial t} + \frac{\partial \rho S_i}{\partial t} = \nabla(\theta \mathbf{D}_i \nabla c_i) - \nabla(\mathbf{q} \nabla c_i) + S c_{s,i} + r_i \quad (9)$$

Where:

- M: mass unit after preference;
- $i = 1, \dots, N$ (N being the number of components);
- c_i : concentration in the aqueous phase [M/L³];
- s_i : concentration in the solid phase [M/M];
- θ : volumetric water content [L³/L³];
- ρ : soil bulk density [M/L³];
- D_i : effective dispersion tensor [L²], components include molecular diffusion, longitudinal and transverse dispersion;
- q : volumetric flux density [L³/L²T];
- S : source-sink term [L³/L³T];
- $c_{s,i}$: concentration of the source-sink [M/L³];
- r_i : reaction term [M/L³T].

When solid- and liquid phase concentrations are at equilibrium they can be related with linear adsorption isotherms, either Freundlich's or Langmuir's. HYDRUS can also consider the physics of non-equilibrium transport by dividing the liquid phase into flowing and stagnant regions. The solute exchange in between the regions is modeled as a first-order process (Langergraber and Simunek, 2005).

2.3 COMPONENTS AND PROCESSES

There are 12 components of the HYDRUS wetland module CW2D, with (Langergraber and Simunek, 2005) (dry weight of the filter material is denoted DW, liter is denoted l):

- SO: dissolved oxygen [mg_{O2}/l];
- CR: readily biodegradable chemical oxygen demand [mg_{COD}/l];
- CS: slowly biodegradable chemical oxygen demand [mg_{COD}/l];
- CI: inert chemical oxygen demand [mg_{COD}/l];
- HE: heterotrophic microorganisms [mg_{COD}/l];
- NS: Nitrosomonas spp. (autotrophic bacteria 1) [mg_{COD}/(gDW)];
- NB: Nitrobacter spp. (autotrophic bacteria 2) [mg_{COD}/(gDW)];
- NH4N: ammonium, NH₄⁺ and ammonia, NH₃ [mg_N/l];
- NO2N: nitrite, NO₂⁻ [mg_N/l];
- NO3N: nitrate, NO₃⁻ [mg_N/l];
- N2: dinitrogen gas, N₂ [mg_N/l];
- IP: inorganic phosphorus [mg_P/l].

There are also nine processes of the HYDRUS wetland module CW2D (Langergraber and Simunek, 2005):

- Hydrolysis, the conversion of slowly biodegradable organic matter (CS) into readily biodegradable organic matter (CR), with a small fraction being converted into inert organic matter (CI). Ammonium is released and it is assumed that no energy utilization is involved in the process;

- Aerobic growth of HE, which leads to formation of biomass;
- Nitrate-based growth of HE on readily biodegradable organic material, supporting denitrification;
- Nitrite-based growth of HE on readily biodegradable organic material, also supporting denitrification;
- Aerobic growth of NS on ammonium, which involves the first step of nitrification;
- Aerobic growth of NB on nitrite, which involves the second step of nitrification;
- Lysis of HE, NS and NB (which are regarded as one process each). The lysis is the sum of all decay and loss processes where microorganisms are involved.

2.4 APPLIED NUMERICAL METHODS OF HYDRUS

To solve the flow equation (4), the Galerkin finite element method is applied. Initial conditions and boundary conditions needs to be specified for the method to proceed. These are given by the user in the user-friendly interface of HYDRUS. The continuous partial differential equation becomes discretized and a grid consisting of triangular (2D) or tetrahedral (3D) elements is introduced to the flow region. The corners of the triangular shapes are the nodal points. A great advantage of the method is that a nonhomogeneous grid can be set; the grid can be made finer where the solution requires higher accuracy. The procedure of the Galerkin finite element method gives as result a system of time-dependent ordinary differential equations with nonlinear coefficients. In order to integrate this system, an implicit finite difference scheme is used. Due to the highly nonlinear nature of this scheme, an iterative process must be performed to obtain solutions at each new time step. The Galerkin finite element method is also applied to solve the solute and heat transport equations, also requiring initial and boundary conditions (Simunek, J. and van Genuchten, M.Th. and Sejna, M., 2006).

3. METHOD

The modeling in HYDRUS was performed with support from a tutorial for the HYDRUS wetland module given by Gunther Langergraber, Habilitation for Sanitary Engineering, during a crash course of the model in BOKU, Vienna. An experimental set up with the filter materials was put in use to provide flow measurements for calibrating soil hydraulic parameters and support the validity of the modeling results. Empirical data concerning nutrient concentrations was not collected but obtained from previous experiments conducted by Dalahmeh (2011).

3.1 MATERIAL

The software used for the computer modeling was HYDRUS supplemented by the Constructed Wetland Module. The modeled results and the experimental data were handled with the free soft-ware products, Notepad ++ and R (version x64 2.14.2).

For the empirical experiment, a set-up of filters constructed during the foregoing research project was used. The experimental setup consisted of 6 columns filled with filter material. These were connected to a pumping system which provided water for irrigation of the filter material. A heater was furthermore connected to the pumping system in order to adjust the temperature of the water before irrigation (Figure 2). Regular tap water was used.

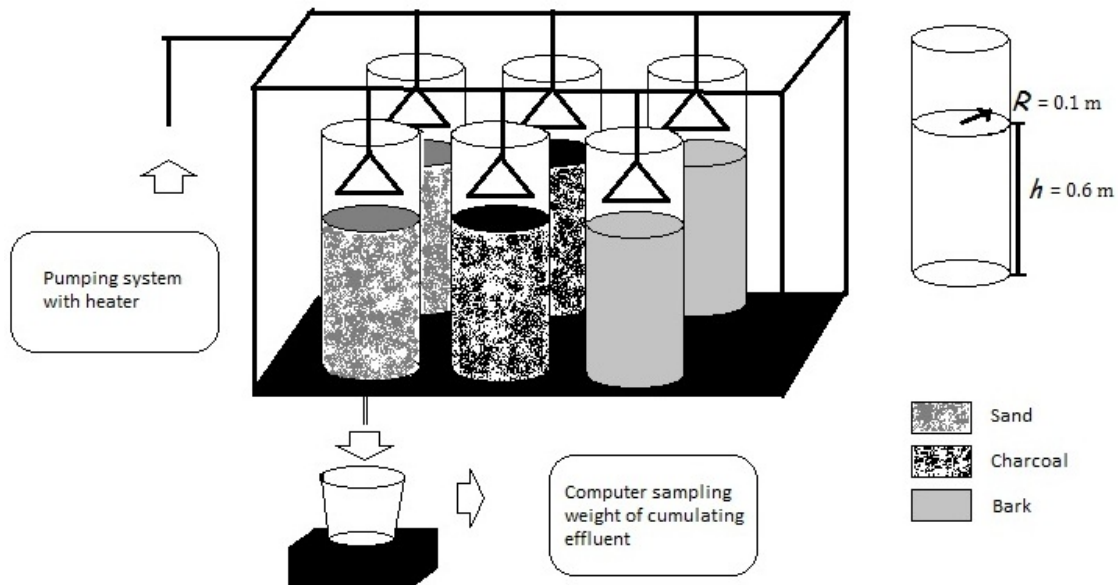


Figure 2 Experimental setup, consisting of a pumping system with heater irrigating tap water into 6 columns filled with filter material. The tap water proceeds through the filters and discharges into a bucket standing on top of a scale. The scale weighs the bucket once every minute and a computer connected to the scale saves this value into a text file, recording also the date and time.

The columns were 1 meter in height and had a diameter of 0.2 meters. The columns were filled with filter material to a level of 0.6 meters. Placed on top of the filter material were some large pieces of gravel. Also at the bottom, coarse gravel was positioned to facilitate the outflow.

Three different filter materials were used in the experimental set-up: pine bark; activated charcoal and sand. Characteristics of the filter materials are summarized in Table 1. Two of the six columns were filled with sand, labeled SAND1 and SAND2; another two with charcoal, labeled CHAR1 and CHAR2; and the last two with bark, labeled BARK1 and BARK2.

Table 1 Characteristics of the bark, charcoal and sand filter materials used in the experiment set up (Dalahmeh et al., 2012)

Parameter	Bark	Charcoal	Sand
pH [SU]	5.1	10.4	7.9
Loss on ignition [%]	90	90	<1
Effective size [mm]	1.4	1.4	1.4
Uniformity coefficient [-]	2.3	2.3	2.2
Bulk density [kg/m ³]	365	283	1690
Particle density [kg/m ³]	1340	1900	2570
Porosity [%]	73	85	34
Surface area [m ² /g]	0.734	>1000	0.136
Hydraulic conductivity [cm/hour]	330	500	360

The filters were irrigated by sprinklers and at the bottom the effluent passed through a plastic pipe into a bucket. The bucket was placed on top of a digital scale connected to a computer into where the weight was recorded once a minute, recording the cumulated effluent flow continuously (Figure 2).

3.2 DATA COLLECTION

The measuring was conducted on one filter at a time. The duplicate of the filter undergoing measurement with the scale was also subjected to irrigation, while the other filter types were let at rest. The irrigation was left running for two weeks, following an intermittent loading scheme: 0.7 liters at time 9:00; 0.2 liters at time 16:00 and 0.1 liter of water at time 20:00. The loading time was fairly short, the water coming as a flush. The specific amounts were chosen because they matched a hydrograph for grey water generation in a typical household in a rural community in Jordan (Dalahmeh, et al., 2012). A steady-state condition in the filters was achieved in 2-3 days of irrigation. Four to five days continued irrigation provided steady state measurements of the cumulated effluent flow from the first filter. Further irrigation for 4-5 days was needed for recording measurements on the duplicate filter. Measurements on all six filters were recorded in equal manner.

Simulation with HYDRUS included different flows (1, 2 and 4 l/day), thus measurements of 1 and 2 l/day loadings were undertaken in the empirical experiment. Measurements of 1 l/day were used to calibrate the model and measurements of 2 l/day loading were used for validation. Since a successful validation was achieved, measurements of 4 l/day loadings were left out (Figure 16). Due to time limitation, measurements on the duplicate filter of each material were left out for the 2 l/day loading regime. One sprinkler was set on SAND1 filter, the other on BARK1. SAND1 was measured for 6 days, after that BARK1 was measured for three days while sprinkler

1 was moved to the charcoal filter. After the three days of measuring BARK1 the scale was moved to measure CHAR1 for another 3 days.

3.2.1 Sprinkler investigation

At the start of the experiment the water flow of the sprinklers was calibrated. The pumping system was connected to a computer where the amount of water and the time of the loading could be specified, using the soft-ware Labview 2009 (National Instrument Sweden AB, Stockholm, Sweden). The sprinklers were calibrated to 0.7 l at time 9:00, 0.2 l at time 16:00 and 0.1 l of water at time 20:00. The amounts were possible to achieve with quite good accuracy. The loading rates of the sprinklers were measured to be around 1.5 l/min. However, due to the elevation of the sprinklers when installed onto the columns, the water flow was slightly reduced. This effect was discovered when less water than anticipated was measured from the bucket during measurement of the first filter type and the conclusion was drawn that a more thorough investigation of the water flow from the sprinklers had to be made.

The amount of water was therefore measured 10 times each for the different loading sizes for sprinkler 1 and sprinkler 2. This data was analyzed statistically using R. First, a check was made to see if the assumption of normal distribution for the values were valid. This was done by calculating and inspecting histograms of the samples, which as a result gave an indication that normal distribution could be assumed even though the number of samples preferably should have been larger. The Student's t-test was performed to determine the mean values and confidence intervals (95%) of the samples.

3.3 HYDRUS MODEL BUILDING

The modeling task consisted of two steps: (i) simulate water flow through the filters using HYDRUS; (ii) simulate the reduction of organic matter and transformation of nitrogen in the filters using HYDRUS wetland module.

3.3.1 Simulating water flow through the filters using HYDRUS

In the HYDRUS environment, modeling essentially consists of:

- **Setting of the geometry/domain of the filters:** the length and width of the column used in the empirical experiment was specified in HYDRUS. Since the filter was of cylindrical shape, a 2D simple geometry with domain option "Axisymmetrical Vertical Flow" was used as setting. This means the calculations were performed on a 2D rectangular layer of the filter (Figure 3).
- **Setting/selection of filter media:** the soil hydraulic parameters to be specified to define the filter media was the saturated soil water content, θ_s , and the saturated hydraulic conductivity, K_s . The set values are shown in Table 2.
- **Setting the loading precipitation rates, evaporation rates, times and duration of loadings:** the loadings were specified in HYDRUS as variable boundary conditions. HYDRUS requires time [hour] and precipitation [cm/h] to describe the loadings. The values used are displayed in Table 3.

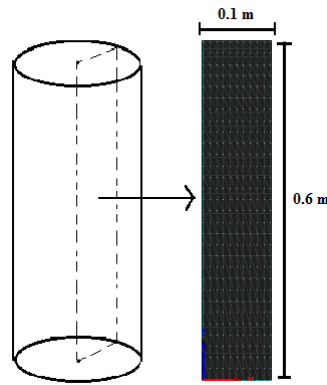


Figure 3 Simple 2D rectangular domain, displayed with grid as it appears in HYDRUS interface.

Table 2 Water flow parameters

Parameter	Bark	Charcoal	Sand
θ_s [-]	0.73	0.85	0.34
K_s [cm/hour]	330	500	360

In the empirical experiment, mentioned above, there was an observation of water splashing up on the walls of the columns. This wetting of the column wall and the filter surface resulted in a small amount of the loading never going through the filter material, instead directly evaporating into the air. This has been taken into account in the simulation by a slight reduction in the duration of loading. The size of the resulting loss was about 8 % of the total loading per day, and this was taken into account in the value for precipitation given in Table 4. Also, due to the observation in the empirical experiment that the effluent water was of a smaller amount than anticipated from the loadings, evaporation was introduced to the Time Variable Boundary Conditions. At first, the difference between amount of water loaded onto the filters and amount of effluent water was assumed to be evaporated. Also it was assumed that the evaporation would be of equal size throughout the day. Although, the numbers calculated from this could not be used in HYDRUS because of numerical issues, somehow it resulted in values closing in on infinity causing the simulation to crash. With some trial and error runs a lesser evaporation could be introduced into the Time Variable Boundary Conditions as seen in Table 3.

Table 3 displays the values as they were inserted into the HYDRUS settings. Since the simulations were run over a timespan of several days, hour was convenient to use as unit. However, during the irrigation the water came as a flush and the duration of the loading was less than a minute. Hence a very small time step (0.0001) was needed to properly describe the loading and the resulting values had to be used with a great number of decimals.

Table 3 Time variable boundary conditions

Time [hour]	Precipitation [cm/hour]	Evaporation [cm/hour]
0.0068	290.299	0.013
7	0	0.01
7.001	290.299	0.013
11	0	0.01
11.002	290.299	0.013
24	0	0.005

3.3.2 Calibrating the model by tuning empirical coefficients

HYDRUS offers the possibility of performing an inverse simulation using measured data points, allowing for soil hydraulic parameters to be estimated. However, when this was tried on the data from the empirical experiment HYDRUS continuously crashed during calculations. Hence, instead of using the built-in inverse simulation, the empirical coefficients α , n and l present in Equations 6-8 as the inverse of the air entry value (α , [L^{-1}]), pore size distribution index (n , [-]) and pore connectivity parameter (l , [-]), were varied throughout a series of simulations.

During the calibration process, each coefficient was modified while the other coefficients were kept constant. α was examined for values between 0.048 and 0.29, n was varied between 2 and 4 and l was examined for values ranging between -0.5 to 1.5. The empirical coefficients were varied independently for each filter material in order to find best fit to measured data.

3.4 REACTIVE TRANSPORT MODELING

In previous research (Dalahmeh et al., 2011) investigation on the filter materials regarding their greywater treatment performance were carried out using the experimental set-up with 6 filters. Artificial greywater was fed to the filters and measurements on the resulting effluent concerning concentrations of nutrients and organic material were taken. The hydraulic loading rate was set to 32 l/m²day and the organic loading rate was set to 14 g BOD₅/m²day. The experiment proceeded for 113 days. The results gained from this experiment were available to use for the reactive transport modeling. The reactive transport modeling was hence designed to correspond to the precedent empirical experiment, using the same hydraulic and organic loading and setting up a simulation time span of 113 days.

When a proper flow model had been established, it was used as a basis when setting up the reactive transport simulation. Default values for transport and reaction parameters were used and the main task in the model building was to specify influent concentrations in the time variable boundary conditions. There were 12 components for which this needed to be done; the most important ones are displayed in Table 5. The values used were chosen to match the characteristics of the greywater which was used for the precedent research project. Measurements of concentrations in the artificial greywater are displayed in Table 4.

Table 4 Influent greywater characteristics

Parameter	Concentration in influent [mg/l]
COD	885
BOD5	425
NO3N	1.08
NH4N	0.46
TN	75.45
PO4P	2.07
TP	4.2

Some assumptions were made to adjust the concentrations in Table 4 to values of the components in CW2D. COD in CW2D is divided in to three categories: readily biodegradable soluble COD (CR); slowly biodegradable soluble COD (CS) and inert soluble COD (CI). It was assumed that CR was equal to the measured BOD5 (Table 4). To determine CS, BOD_u was considered since BOD_u can be assumed to equal the total amount of biodegradable COD (Ghunmi, 2011). It was assumed that BOD_u could be determined from the measured BOD5 by dividing BOD5 with a factor 0.7. This factor was decided based on literature values (Ghunmi, 2011). Using this factor, the calculation of CR, CS and CI was done by:

$$CR = BOD5 \quad (10)$$

$$CS = BOD5/0.7 - CR \quad (11)$$

$$CI = COD - CR - CS \quad (12)$$

There are also three different forms of nitrogen in CW2D: NH4N (representing ammonium and ammonia); NO2N and NO3N. In CW2D the organic nitrogen is included in the CR, CS and CI. Measured values of NH4N and NO3N were available to use, the influent concentration of NO2N was assumed to be zero. The nitrogen content of CR, CS and CI was adjusted in the model so that it would correspond to the measured organic nitrogen:

$$OrgN = TN - NH4N - NO3N \quad (13)$$

The measured PO4P was used as IP. It was assumed that subtracting the measured PO4P from the measured total phosphorus (TP) would equal the amount of organic phosphorus. In CW2D the organic phosphorus is modeled as part of the CR, CS and CI. The phosphorus content of CR, CS and CI was adjusted in the model so that it would correspond to the measured organic phosphorus. The values used for simulation are displayed in Table 5.

Table 5 Influent concentrations used for time variable boundary conditions

Component	Concentration [mg/l]
CR	425
CS	180
CI	278
NH4N	0.46
NO2N	0
NO3N	1.08
N2	0
IP	2.07

Initial values for concentrations in the filter were assumed to be zero, which corresponds to a completely “clean” filter at startup. All parameters regarding solute transport were set to the standard literature values.

4. RESULT PART I: FLOW EXPERIMENTS AND SIMULATION

4.1 SPRINKLER INVESTIGATION

The result of the sprinkler investigation showed that the observed values were lower than the set values but the confidence intervals were slim, suggesting that the amount loaded did not vary to a great extent from the observed value (Table 6).

Table 6 Result of student's t-test on water flow measurements

Set value	Observed value [ml]	Confidence interval (95%)
Sprinkler 1, 0.7 l	655.4	(652.7, 658.0)
Sprinkler 2, 0.7 l	655.4	(653.1, 657.7)
Sprinkler 1, 0.1 l	95.3	(94.7, 95.9)
Sprinkler 2, 0.1 l	96.8	(96.3, 97.4)
Sprinkler 1, 0.2 l	188.1	(187.6, 188.5)
Sprinkler 2, 0.2 l	188.6	(188.1, 189.0)

Furthermore, results using Levene's test showed that the variances of sprinkler 1 and sprinkler 2 were homogenous for all amounts. This information was further used in a two sample version of Student's t-test to check whether the mean values of the two sprinklers could be seen as significantly similar. The obtained p-values for the 0.7 l loading and the 0.2 l loading were greater than the chosen significance level 0.05, hence the equality of those mean values could be accepted. However, the p-value for the 0.1 l loading was 0.0007 and the null hypothesis (similar mean values) had to be rejected for this amount.

It was also observed that the rather strong flow from the sprinklers resulted in scattering of the water up against the column walls. The distance between the filter surface and the sprinkler influenced this behavior and in the set-up consideration was taken into placing the sprinklers so that the water scattering would be minimized; nonetheless it still occurred to some extent.

4.2 RESULTS: EMPIRICAL EXPERIMENT

4.2.1 Bark filter

The water flow in the bark filters showed a slightly larger spread in water flow compared to the charcoal filters (Figure 4).

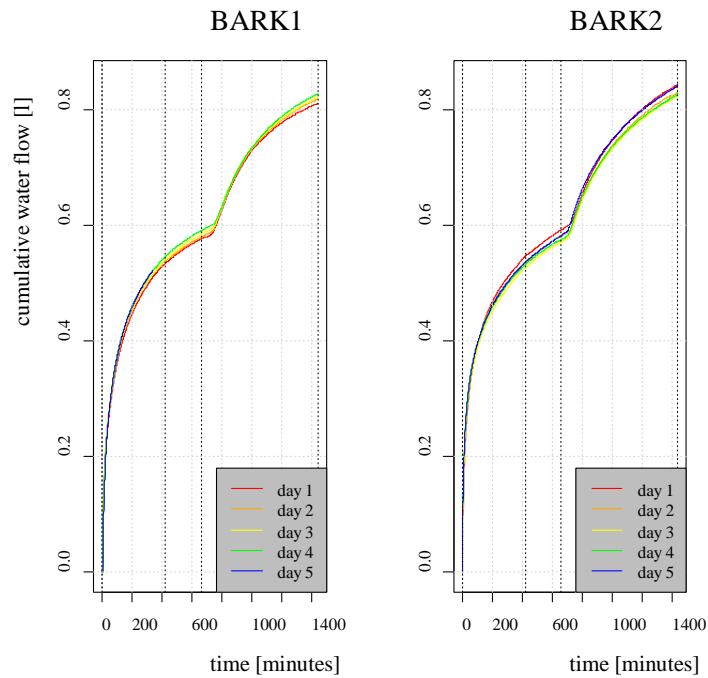


Figure 4 The filters BARK1 and BARK2 over time. The data was separated and made noncumulative from day to day to enable comparison of flow behavior each day.

Data was compared for the two four day runs of the bark filters. The cumulative water flow in the two bark filters seems to behave fairly similar even though it was noticed that BARK1 was accumulating less water than BARK2 (Figure 5).

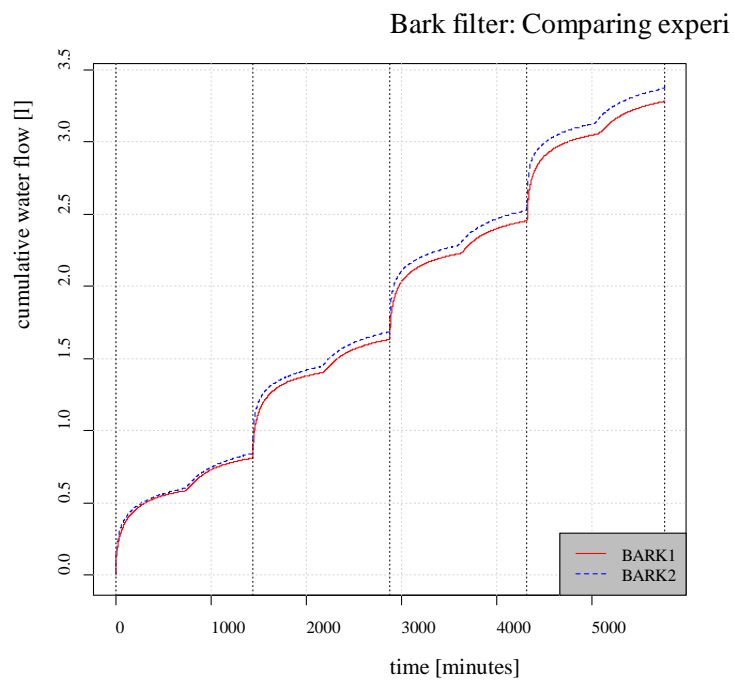


Figure 5 The cumulative water flow in the filters BARK1 and BARK2 during the 4 days of measurement.

The average amount of water coming out of the filters per day was 820 ml for BARK1 and 837 ml for BARK2, even though they were each loaded with approximately 940 ml. The bark filters produced a dark tea colored effluent with no visible particles.

4.2.2 Charcoal filter

The water flow in the charcoal filters behaved similarly to that of the bark filter. The second charcoal filter, CHAR2, showed a wider spread between days mainly because of day 3 measurements (Figure 6).

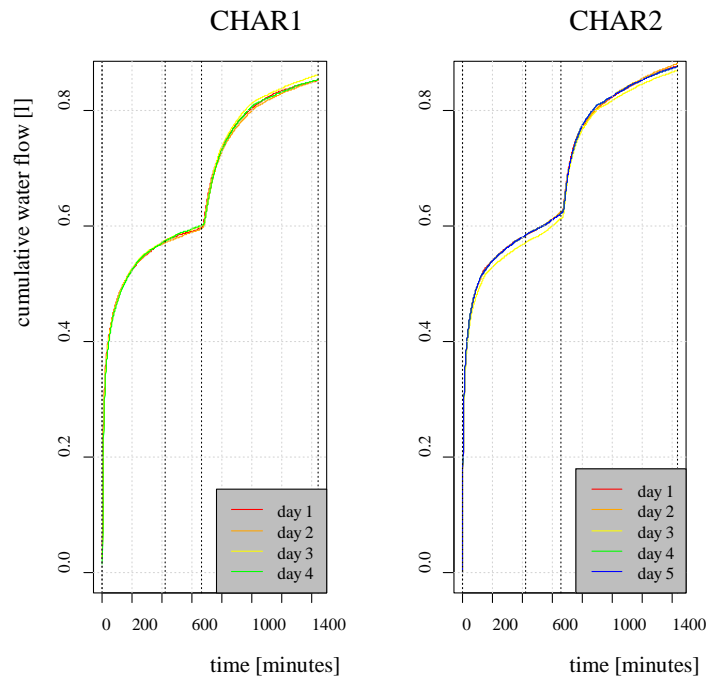


Figure 6 The cumulative water flow in charcoal filters CHAR1 and CHAR2 over time. The data was separated and made noncumulative from day to day to enable comparison of demonstrated flow each day.

CHAR2 was observed to release more effluence water than CHAR 1 when comparing the cumulated effluent flow spanning over four days of measuring (Figure 7).

Charcoal filter: Comparing ex

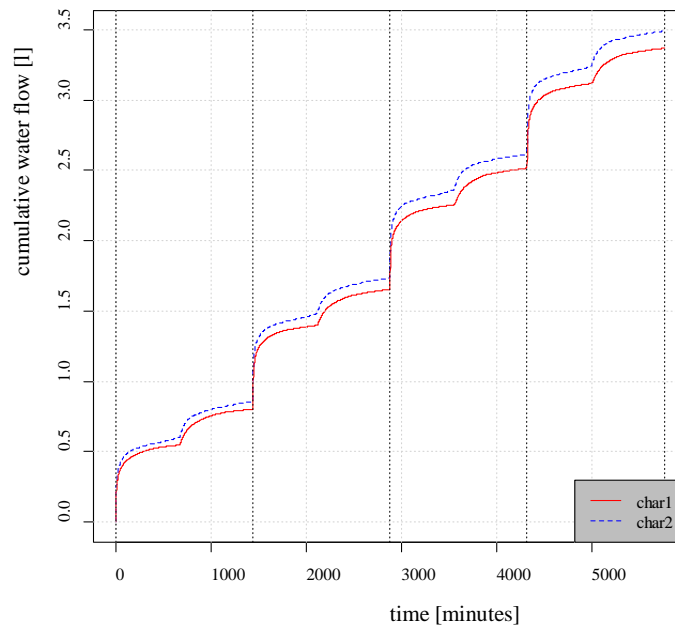


Figure 7 Measured data from the filters BARK1 and BARK2 during the 4 days of measurement.

The average amount of water discharged from filters per day was 854.3 ml for CHAR1 and 875.0 ml for CHAR2, even though they were each loaded with approximately 940 ml.

The effluent water from the charcoal filters, when examined in the bucket, was clear and without particles. If observed carefully a slight amount of coal dust could be seen at the bottom of the buckets.

4.2.3 Sand filter

The water flow in the sand filter was demonstrated to be consistent from day to day (Figure 8). Some disturbances to the measurement of SAND1 occurred during day 3 and 4 (Figures 8-9).

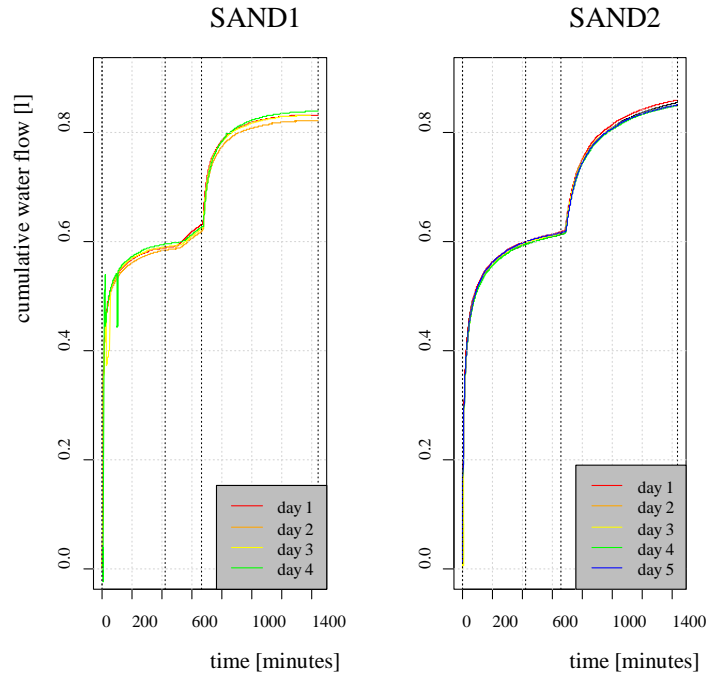


Figure 8 The filters SAND1 and SAND2 over time. The data was separated and made noncumulative from day to day to enable comparison of demonstrated flow each day.

The filters SAND1 and SAND2 displayed an equal behavior to the bark and charcoal filters, with the exception of a change to linear behavior in SAND1 immediately before the third loading (Figure 8).

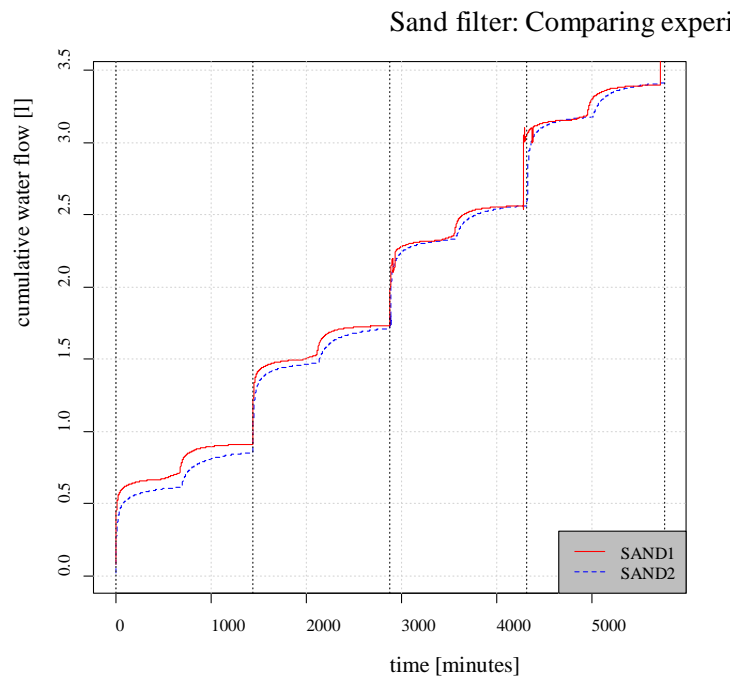


Figure 9 The filters SAND1 and SAND2 during the 4 days of measurement.

Less water was discharged from the filters than expected. The amount of effluent water was 852 ml per day (average taken from SAND2) although the total amount of water loaded per day was approximately 940 ml.

The effluent water from the sand filters was upon inspection clear, containing no visual particles.

4.2.4 Comparison between filters

Some variation in the water flow of the duplicate filters of the same type was observed. The bark filters seemed to display the least difference when compared to each other, while CHAR1 and CHAR2 demonstrated the greatest difference (Figure 10).

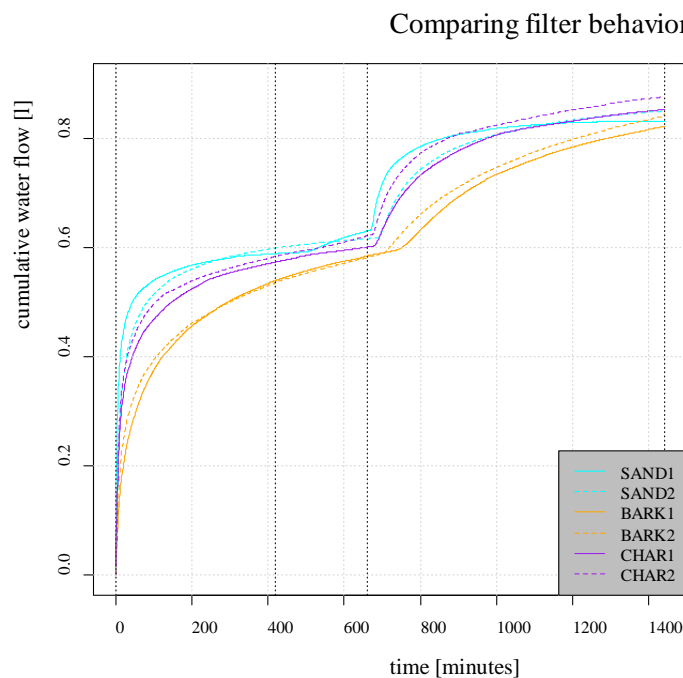


Figure 10 The cumulative water flow for all filters, including duplicates for the same filter types.

The sand filter seemed to have the fastest flow while the bark material resulted in the slowest flow. The amounts of effluent water at the end of the day varied; CHAR2 released the largest amount of effluent water while the bark filters had the smallest amount (Figure 10).

4.3 CALIBRATION RESULTS

When configuring the empirical coefficients, different sets of values of coefficients l , n and α , gave a broad variety to the outcome of simulated data (Figure 11). Using a smaller value of α gave a steeper curve for the cumulative water flow, also giving it a bulging appearance. For higher values of l the cumulative water flow was lowered. When the other exponent, n , was varied unrealistic results were demonstrated for smaller values (cumulative water flow was increased much). Higher values were demonstrated to lower the cumulative water flow, although not as drastically as l .

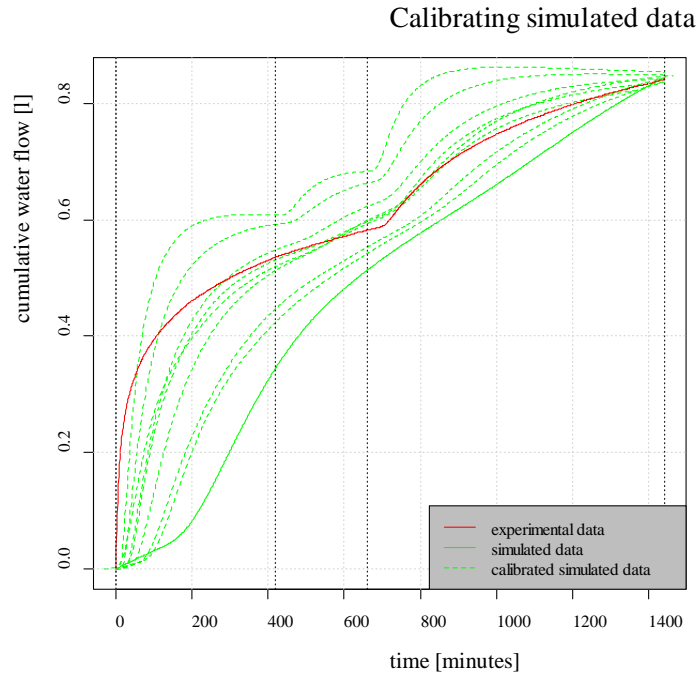


Figure 11 The cumulative water flow over time for measured and simulated data, calibrating the simulated data to fit experimental data by varying the empirical coefficients l , n and α .

The values which finally were judged to give a good enough fit of simulated data onto the experimental data are presented in Table 7. The values were chosen with regard to best fit by visually comparing plotted simulated and experimental data.

Table 7 Empirical coefficients used in final calibration

Coefficient	Initial values	Bark	Charcoal	Sand
α	0.145	0.048	0.05	0.0725
l	0.5	1	1	1
n	2.68	4	3.1	2.68

4.4 SIMULATED FLOWS

4.4.1 Bark filter

HYDRUS modeled the water flow in the bark filters well when calibration to empirical constants had been performed. The calibration needed was a decrease of the inverse of air-entry value, α , and an increase of the pore-size distribution index, n . As for the other filters, l , the pore-connectivity parameter, was changed to 1 instead of 0.5. The simulation result from the run prior to the calibration did not resemble experimental data well. The simulated water flow was not sufficiently fast to match experimental data for the first loading. Not even with the calibration of model parameters could the speed of water flow through the physical filter be achieved in the simulations (Figure 12).

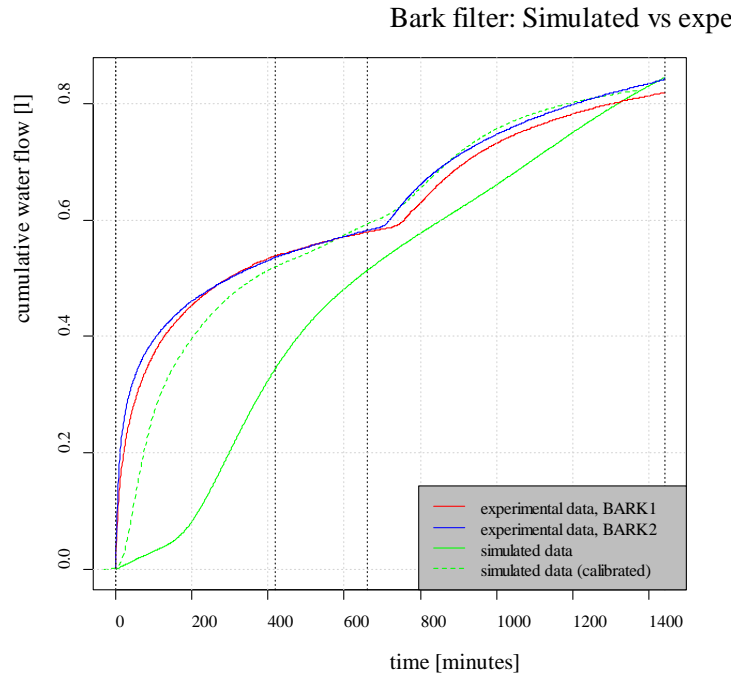


Figure 12 Measured cumulative water flow over time for BARK1 and BARK2 together with simulated data from simulation prior to calibration and simulation with modified empirical coefficients.

4.4.2 Charcoal filter

As with the bark filter, the simulated water flow in the charcoal was not as fast as the measured data (Figure 13).

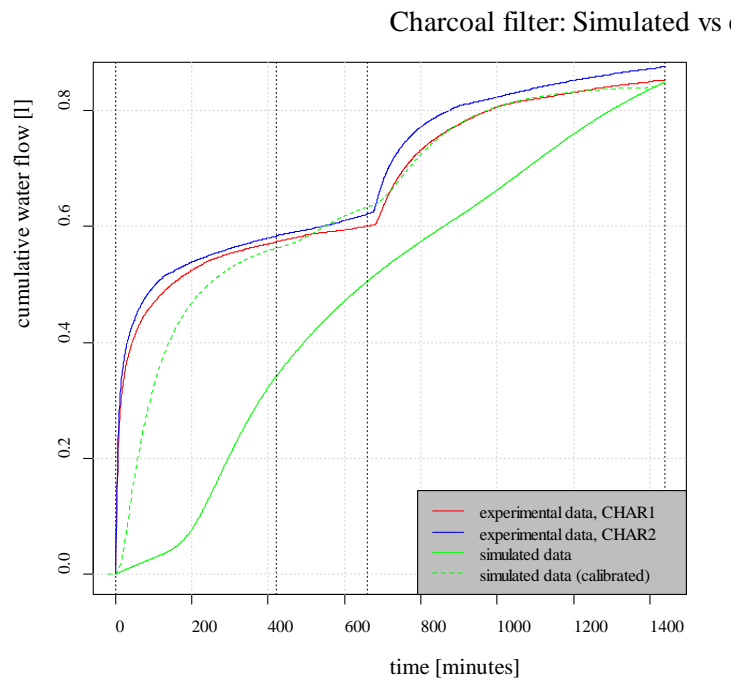


Figure 13 Measured cumulative water flow over time for CHAR1 and CHAR2 together with simulated data from simulation prior to calibration and simulation with modified empirical coefficients.

4.4.3 Sand filter

The simulated cumulative water flow was modeled quite accurately by HYDRUS (Figure 14). The simulated flow after the first loading appeared somewhat slower compared to the measured data. For the second loading, the simulated flow matched the experimental data from filter SAND1 very well. After the third loading the simulated data appeared to follow the flow documented for SAND2, while the flow in SAND1 was slightly quicker.

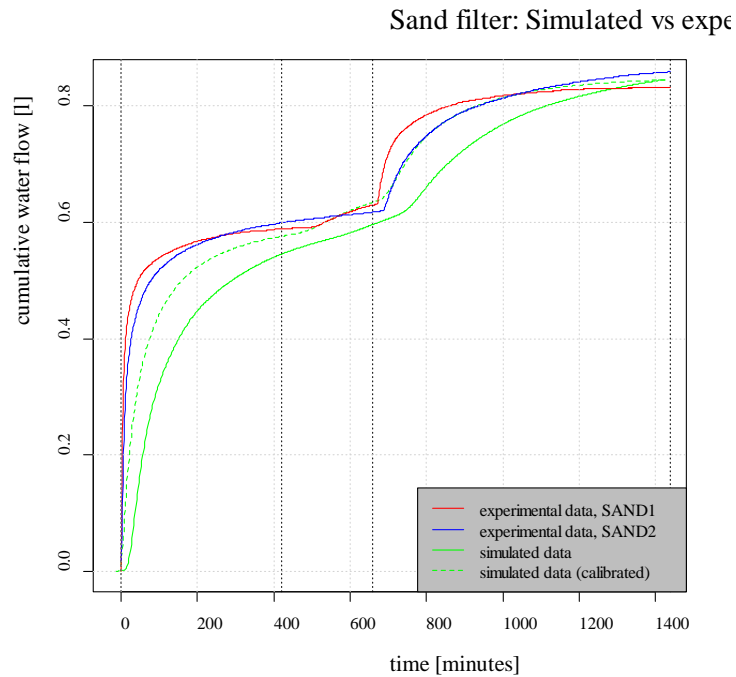


Figure 14 Measured cumulative water flow over time for SAND1 and SAND2 together with simulated data from simulation prior to calibration and simulation with modified empirical coefficients.

4.4.4 Validating estimated empirical coefficients

Simulating flow in the filters with a doubled loading amount, 2 l/day, using the coefficients from Table 7, demonstrated adequate results; the simulated data corresponds well to the data from measurements of the filters using a loading rate of 2 l/day (Figure 15).

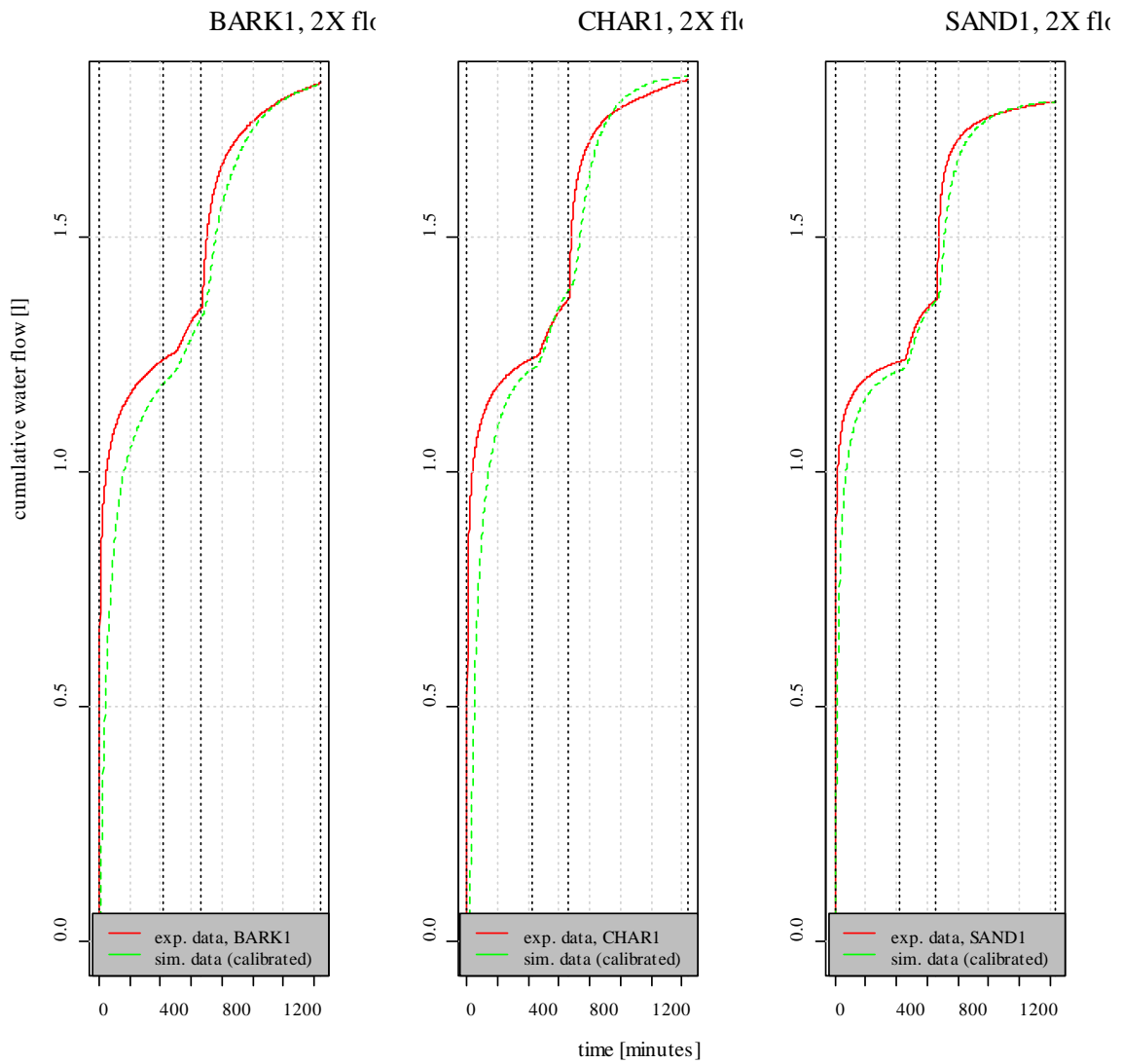


Figure 15 Measured cumulative water flow over time with corresponding simulated data of increased flow from 1 l/day to 2 l/day.

5. RESULT PART II: REACTIVE TRANSPORT SIMULATIONS

5.1 BIOMASS FORMATION

It was observed from the simulations that none of the filters appeared to reach a steady state during the 113 days long simulation since HE appeared to grow continuously. The autotrophic bacteria appeared to reach a steady state of constant growth after 30 days for the sand filter and 50 days for the bark and charcoal filter.

In the simulations, the microorganisms appeared to be mainly concentrated to the top half of the filters, with the largest concentration situated at the top layer of the filter (Figure 16).

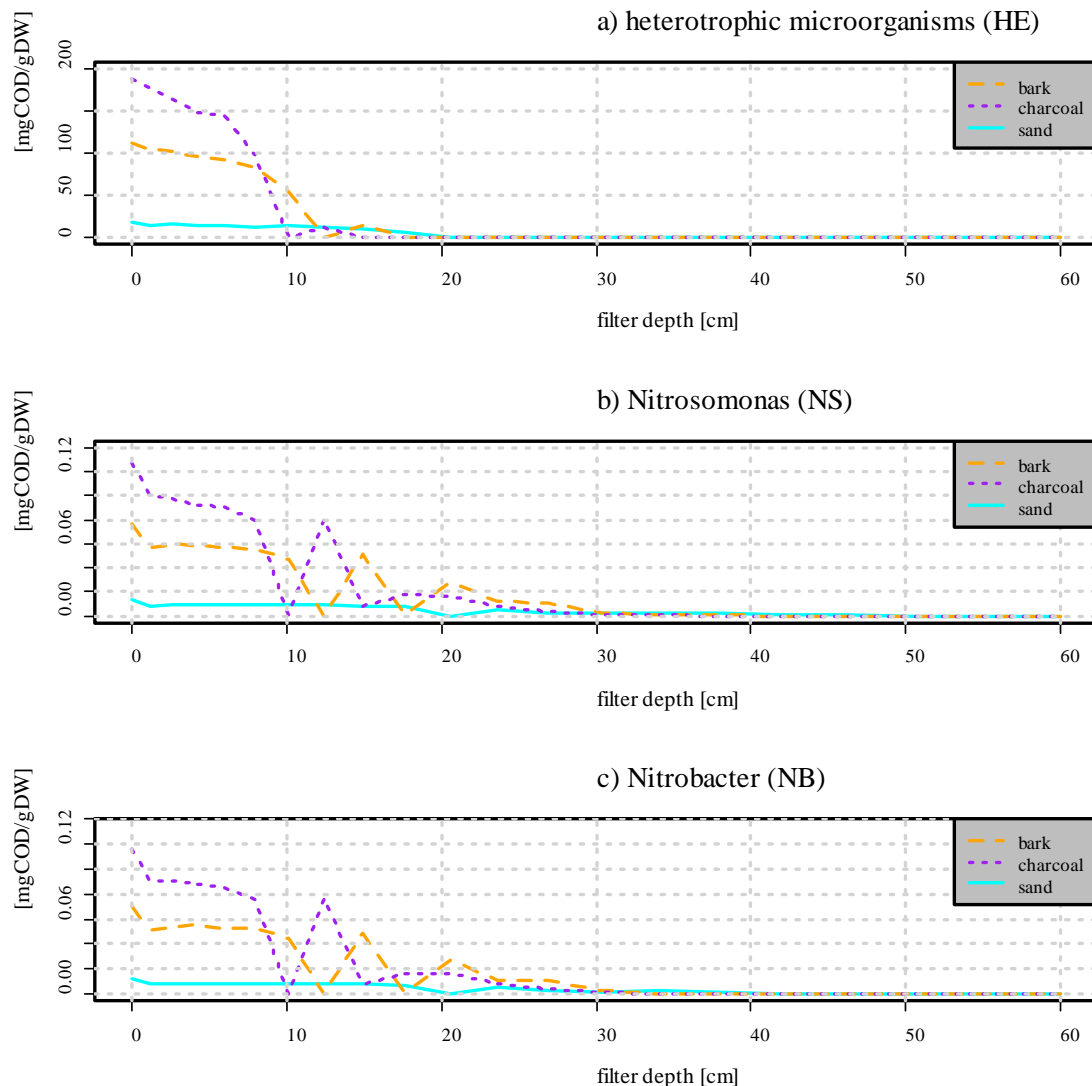


Figure 16 Distribution of microorganisms over filter depth (DW = dry weight of filter material).

In the simulation the charcoal filter appeared to have the largest concentration of HE (0-200 mgCOD/g DW), mainly present in the top 10 cm of the filter (Figure 16 A). The bark filter also displayed a large amount of HE (0-100 mgCOD/g DW), present in the top 20 cm of the filter (Figure 16 A). The simulated sand filter demonstrated a

considerably smaller amount of HE (0-19 mgCOD/g DW) than the bark and charcoal filters (Figure 16 A).

The simulated charcoal filter appeared to have the largest concentration of NS (0-127 $\mu\text{gCOD/g DW}$), and NB (0-116 $\mu\text{gCOD/g DW}$), mainly present in the top 30 cm of the filter (Figure 16 B, C). The bark filter also displayed a large amount of NS (0-76 $\mu\text{gCOD/g DW}$) and NB (0-70 $\mu\text{gCOD/g DW}$), present in the top 30 cm of the filter (Figure 16 B, C). The simulated sand filter demonstrated a considerably smaller amount of NS (0-13 $\mu\text{gCOD/g DW}$) and NB (0-12 $\mu\text{gCOD/g DW}$) than the bark and charcoal filters (Figure 16 B, C). The NS and NB inside the sand filter were present at filter depth 0-50 cm.

5.2 ORGANIC MATTER DEGRADATION

The organic matter degradation could be evaluated from simulated data on organic matter concentrations (Figures 17-19). Since the outgoing concentration of CI was the largest addition to COD in the effluent, CI was also presented in a graph (Figure 19) depicting CI concentration versus filter depth during the last day of the simulation period (day 113).

5.2.1 Readily biodegradable soluble COD

From the simulation it appeared that initially, there was a large outgoing concentration of CR occurring during the first 15 days for the sand filter (0-380 mg/l) and first 20 days for the bark and charcoal filters (0-280 mg/l). After 20 days in the simulation, the outgoing concentration of CR in all filters was approximately zero (Figure 17) even though the influent concentration of CR was 425 mg/l.

Readily biodegr. COD (CR)

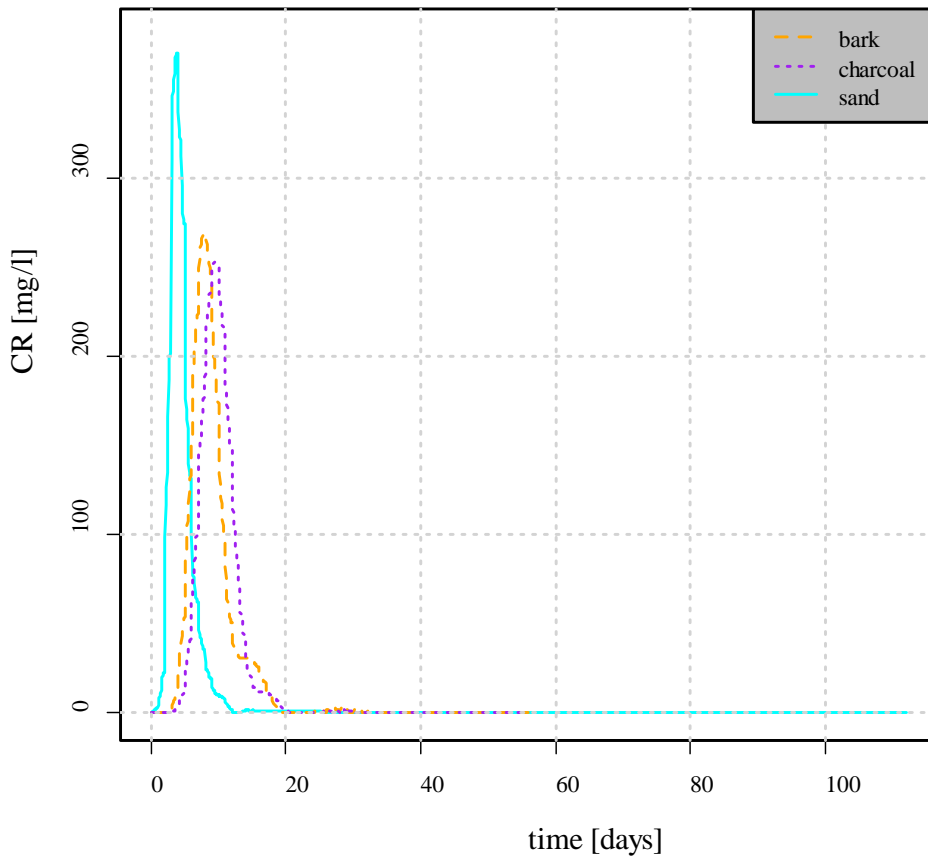


Figure 17 Effluent concentration of readily biodegradable soluble COD (mg/l) over time (days) for the bark, charcoal and sand filter.

5.2.2 Slowly biodegradable soluble COD

The concentration of CS in the effluent of each simulated filter appeared to be close to zero (Table 8). This was a negligible amount compared to the concentration of CS in the influent (180 mg/l).

5.2.3 Inert soluble COD

The simulated concentration of CI in the filter effluent rose quickly from zero at the start up to approximately 310 mg/l 10 days later in each filter (Figure 18). The concentration held steady at 310 mg/l for the rest of the simulation (day 10-113) for each filter. The sand filter appeared to reach the steady concentration of 310 mg/l approximately 5 days earlier than the bark and charcoal filter (Figure 18).

The simulated concentration of CI in the filter effluent (310 mg/l) was slightly larger than the concentration of CI in the influent (275 mg/l).

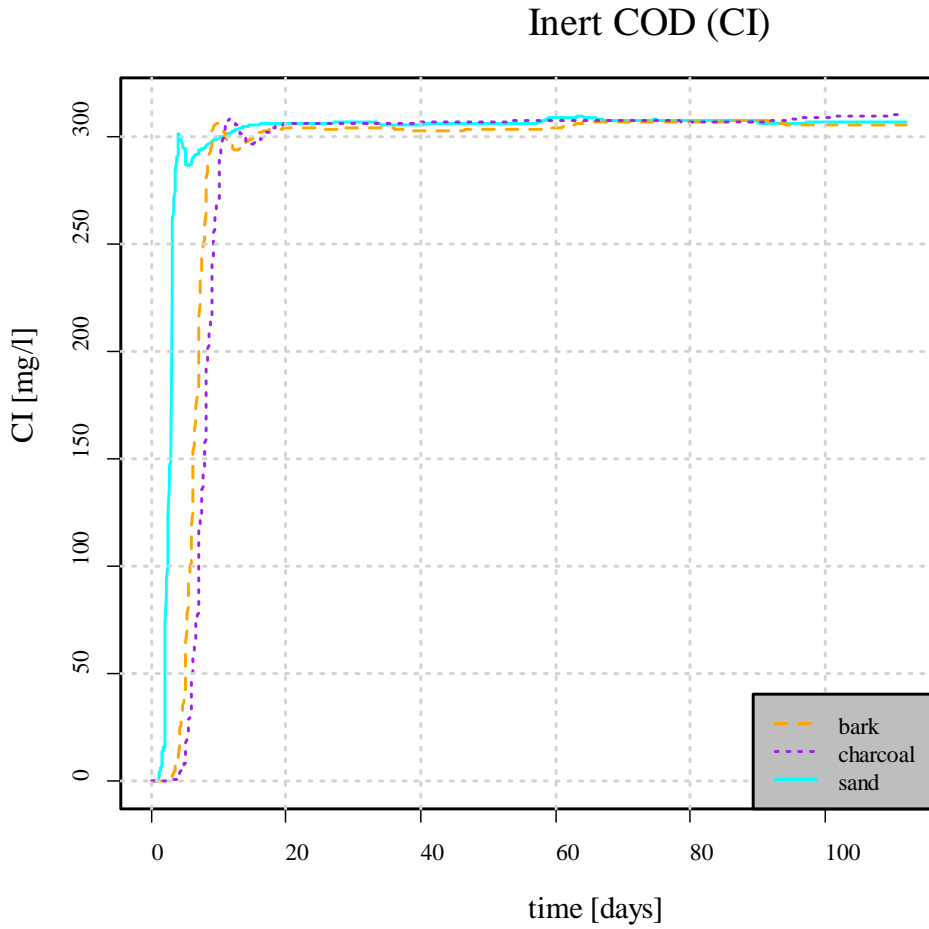


Figure 18 Effluent concentration of inert soluble COD (mg/l) over time (days) for the bark, charcoal and sand filter.

It appeared that the concentration of inert COD throughout the filter depth was approximately 310 mg/l for all three filter types (Figure 19). The immediate top layer of each simulated filter displayed higher concentrations of inert COD (735 mg/l for bark filter, 574 mg/l for charcoal filter and 800 mg/l for sand filter).

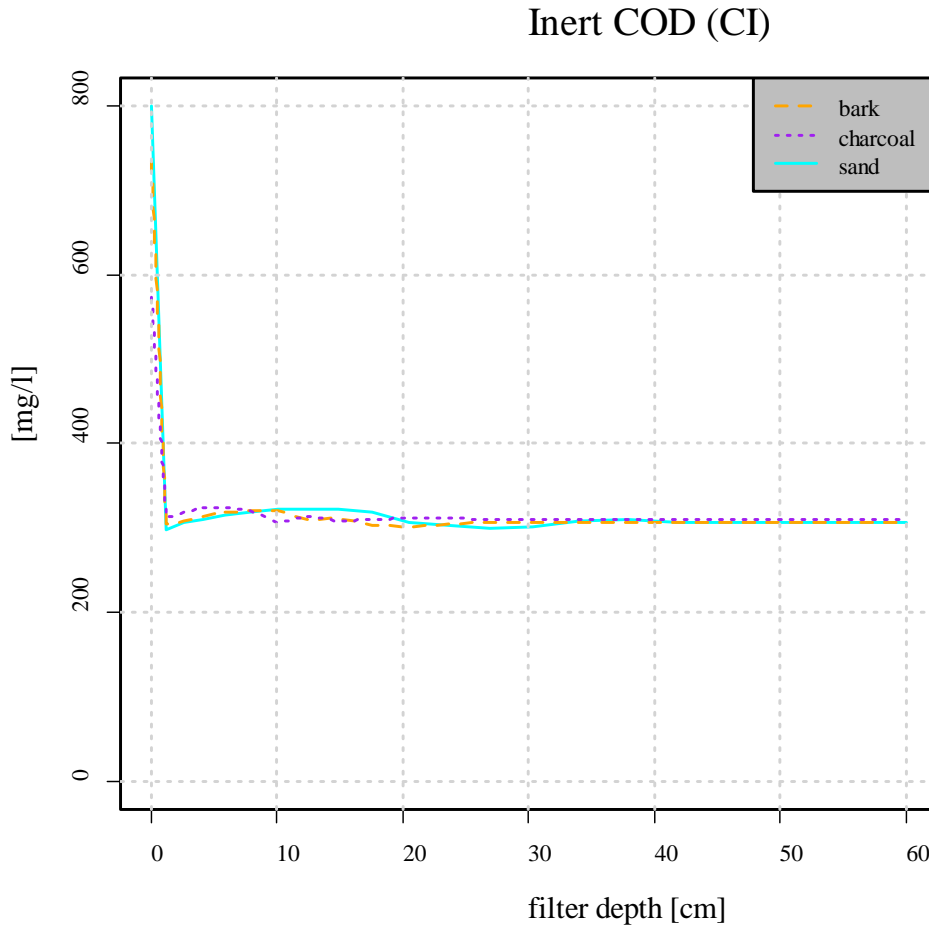


Figure 19 Concentration of inert soluble COD (mg/l) over filter depth (cm) for the bark, charcoal and sand filter during the last day of simulation (day 113).

5.3 INORGANIC PHOSPHORUS CONCENTRATION

The simulated IP effluent concentration appeared not to reach a steady state; instead it was fluctuating for each of the three filters (Figure 20). The effluent concentration of IP in the three different filter types: bark; charcoal and sand, was at the end of the simulation approximately 0.3, 0.1 and 0.4 mg/l respectively (Figure 20).

It appeared from the simulation that the IP concentration in the effluent (0.1-0.4 mg/l) was less than the IP concentration in the influent (2.07 mg/l).

Inorganic phosphorus (IP)

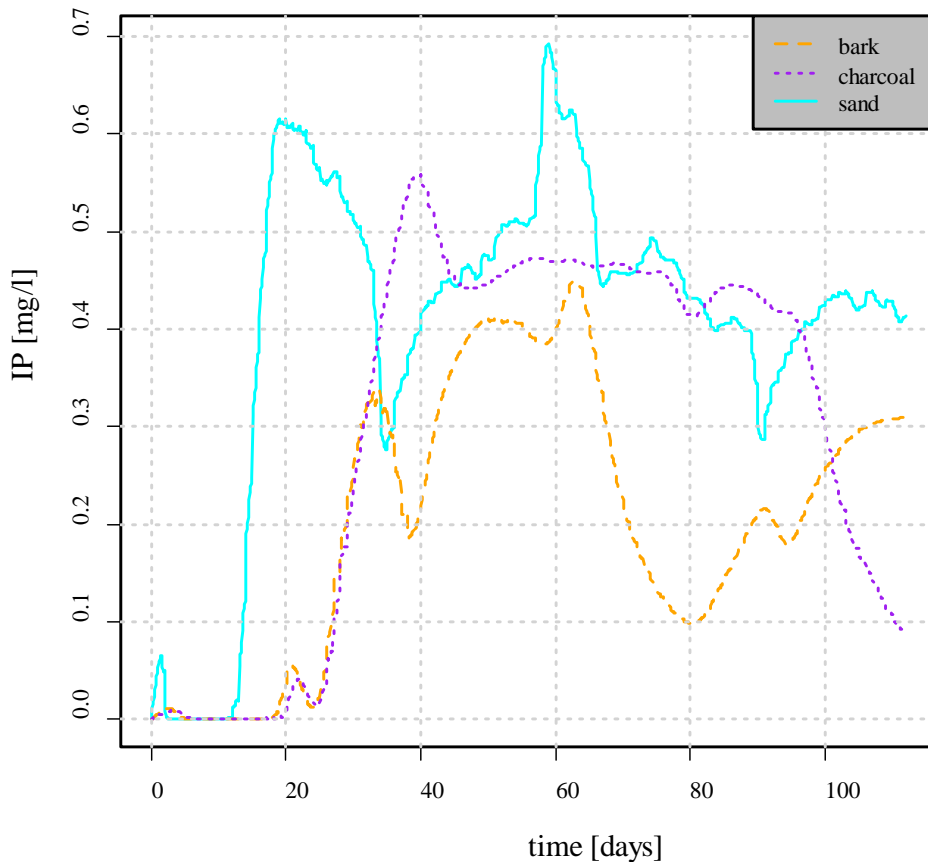


Figure 20 Effluent concentration of inorganic phosphorus (mg/l) over time (days) for the bark, charcoal and sand filter.

It appeared that for the bark filter, the simulated concentration of IP in filter depth 0-20 cm was zero. At 20 cm depth the concentration increased from zero to 0.7 mg/l (Figure 21). Between 20 and 30 cm depth the concentration of IP in the bark filter decreased linearly from 0.7 mg/l to 0.3 mg/l. From 30 to 60 cm depth it appeared that the concentration of IP in the bark filter remained approximately 0.3 mg/l (Figure 21).

The charcoal filter appeared to contain the lowest simulated concentrations of IP. The concentration of IP in the charcoal filter at filter depth 0-15 cm was approximately zero (Figure 21). At 16 cm depth the filter appeared to demonstrate a peak in IP concentration (0.3 mg/l). Between depth 25-60 cm the IP concentration was constant (0.1 mg/l) (Figure 21).

For the sand filter, it appeared that the simulated concentration of IP varied along the flow path between 0 and 40 cm depth (Figure 21). At 5 cm depth there was a peak in IP concentration (3.1 mg/l), followed by zero concentration at depth 6-20 cm. From 20 cm down to 23 cm depth the concentration of IP increased to 1.2 mg/l, which after 23 cm depth decreased to 0.3 mg/l at 40 cm depth. From 40-60 cm depth the concentration of IP in the sand filter was fairly constant (0.45 mg/l) (Figure 21).

Inorganic Phosphorus (IP)

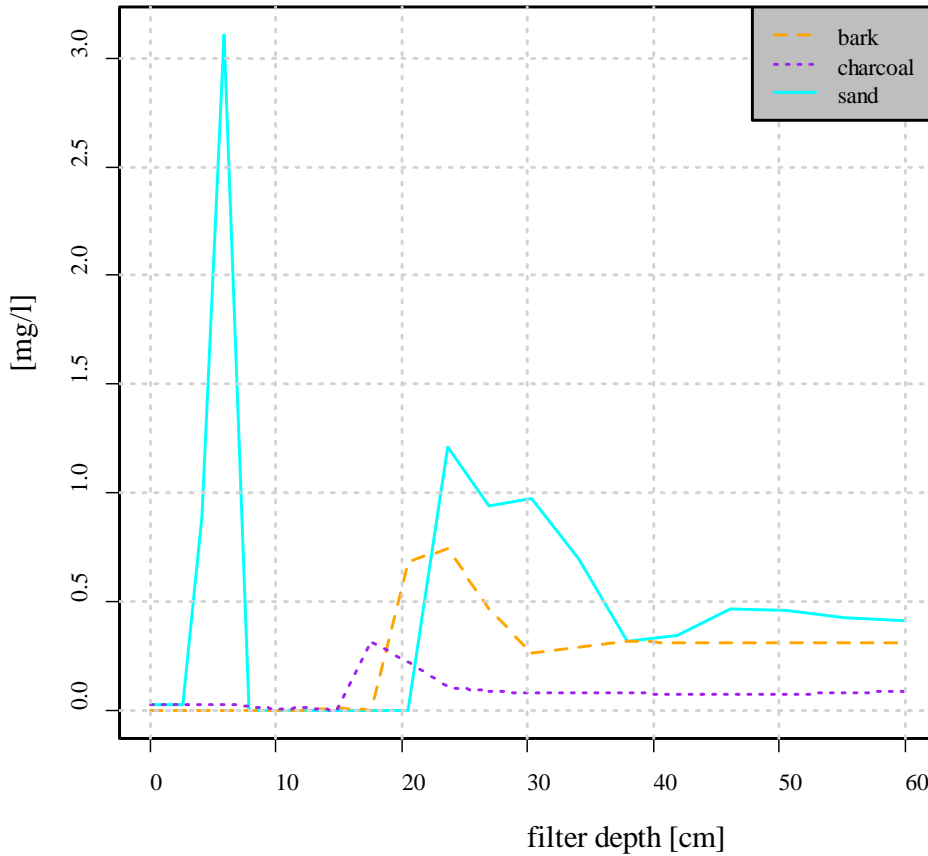


Figure 21 Concentration of inorganic phosphorus (mg/l) over filter depth (cm) for the bark, charcoal and sand filter during the last day of simulation (day 113).

5.4 NITROGEN TRANSFORMATION

Nitrogen transformation could be evaluated from the simulations that provided concentrations of NO_3N , NO_2N , NH_4N and N_2 in the filters. (Figures 22-26). Since the outgoing concentration of NO_3N was the largest fraction of nitrogen in the effluent, NO_3N was also presented in a graph (Figure 19) depicting NO_3N concentration versus filter depth during the last day of the simulation period (day 113).

5.4.1 Nitrate concentration

The simulated concentration of NO_3N in the effluent from the bark and charcoal filters increased from zero at start to approximately 50 mg/l on day 25 (Figure 22). For the rest of the simulation period (day 25-113) the NO_3N concentration in the effluent was constant (50 mg/l) for both bark and charcoal filter (Figure 22).

The simulated concentration of NO_3N in the sand filter effluent increased from zero at start to approximately 47 mg/l on day 12 (Figure 22). For the rest of the simulation period (day 12-113) the concentration of NO_3N in the effluent was constant (47 mg/l) (Figure 22).

The influent concentration of NO₃N was 1.08 mg/l.

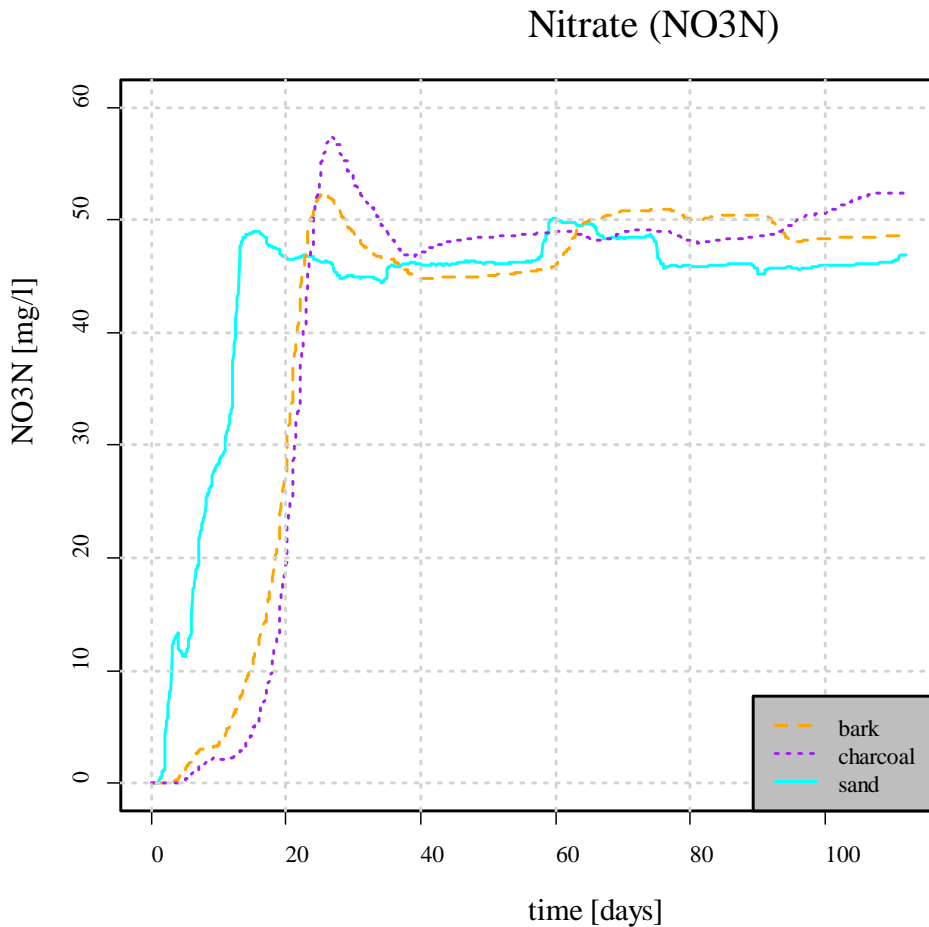


Figure 22 Effluent concentration of nitrate (mg/l) over time (days) for the bark, charcoal and sand filter.

The immediate top layer of each simulated filter displayed high concentrations of NO₃N (106 mg/l for bark and sand filter, 86 mg/l for charcoal filter) (Figure 23). The simulated concentration of NO₃N inside the bark filter varied in the top half of the filter (42-65 mg/l) but held a constant concentration (49 mg/l) in the bottom half (Figure 23).

The simulated concentration of NO₃N inside the charcoal filter varied in the top 20 cm of the filter (46-68 mg/l) but was constant for filter depth 20-60 cm (53 mg/l) (Figure 23).

The simulated concentration of NO₃N inside the sand filter displayed the largest variation: the concentration of NO₃N inside the sand filter varied between 34-70 mg/l in the filter depth 0-40 cm (Figure 23). At filter depths 40-60 cm the concentration was fairly constant (47 mg/l) (Figure 23).

Nitrate (NO₃N)

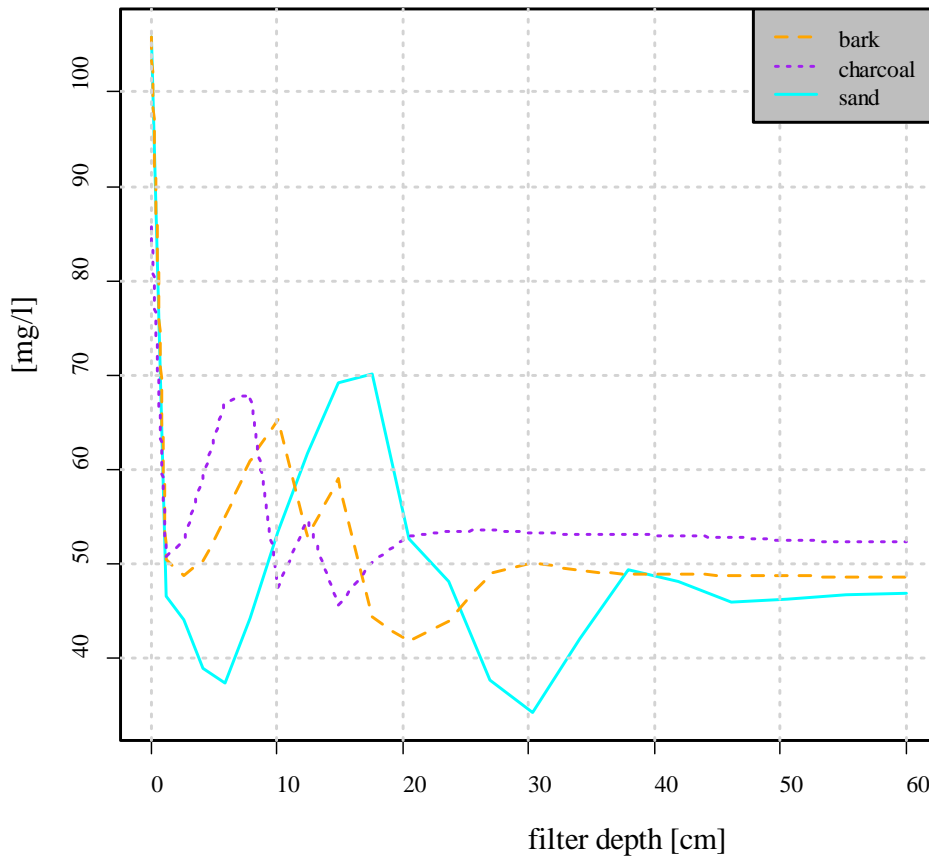


Figure 23 Concentration of nitrate (mg/l) over filter depth (cm) for the bark, charcoal and sand filter during the last day of simulation (day 113).

5.4.2 Ammonium and ammonia concentration

From the simulation it appeared that initially, there was a large outgoing concentration of NH₄N occurring during the first 15 days for the sand filter (0-10 mg/l) and first 25 days for the bark and charcoal filters (0-40 mg/l and 0-45 mg/l respectively) (Figure 24). After 15 days, the simulated sand filter effluent concentration of NH₄N was approximately 0.1 mg/l for the remaining simulation period (days 16-113) (Figure 24). After 25 days, the simulated effluent concentration of NH₄N from the bark and charcoal filter was approximately 0.1 mg/l and 0.09 mg/l, respectively, for the remaining simulation period (days 26-113) (Figure 24).

Ammonium and ammonia (N)

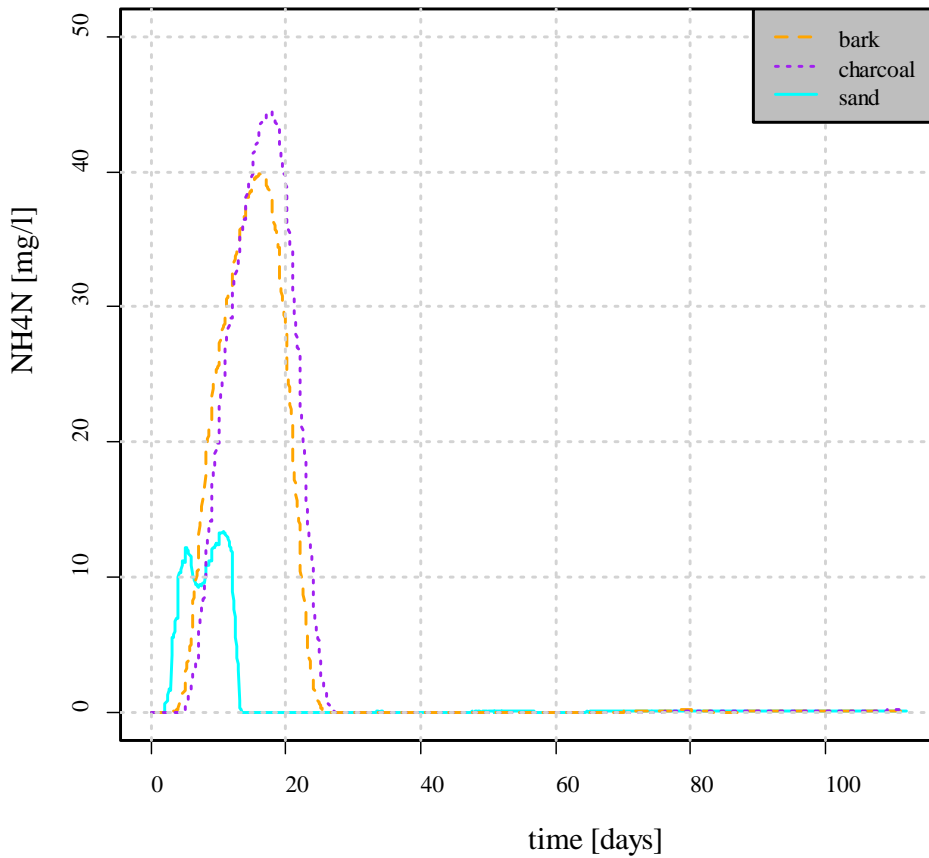


Figure 24 Effluent concentration of ammonium/ammonia (mg/l) over time (days) for the bark, charcoal and sand filter.

5.4.3 Nitrite concentration

The simulated effluent concentration of NO₂N in the sand filter increased from zero at startup to 0.35 mg/l during day 15. From day 15 until the end of the simulation of the sand filter, the outgoing NO₂N concentration appeared as nearly zero (0.025 mg/l) (Figure 25).

The simulated effluent concentration of NO₂N in the bark and charcoal filter increased from zero at start to 0.5 mg/l during day 20. During day 20-25, the outgoing NO₂N concentration of the bark and charcoal filter appeared to decrease rapidly to nearly zero (0.024-0.026 mg/l). From day 25 until the end of the simulation of the bark and charcoal filter, the outgoing NO₂N concentration appeared as nearly zero (0.025 mg/l) (Figure 25).

Nitrite (NO₂N)

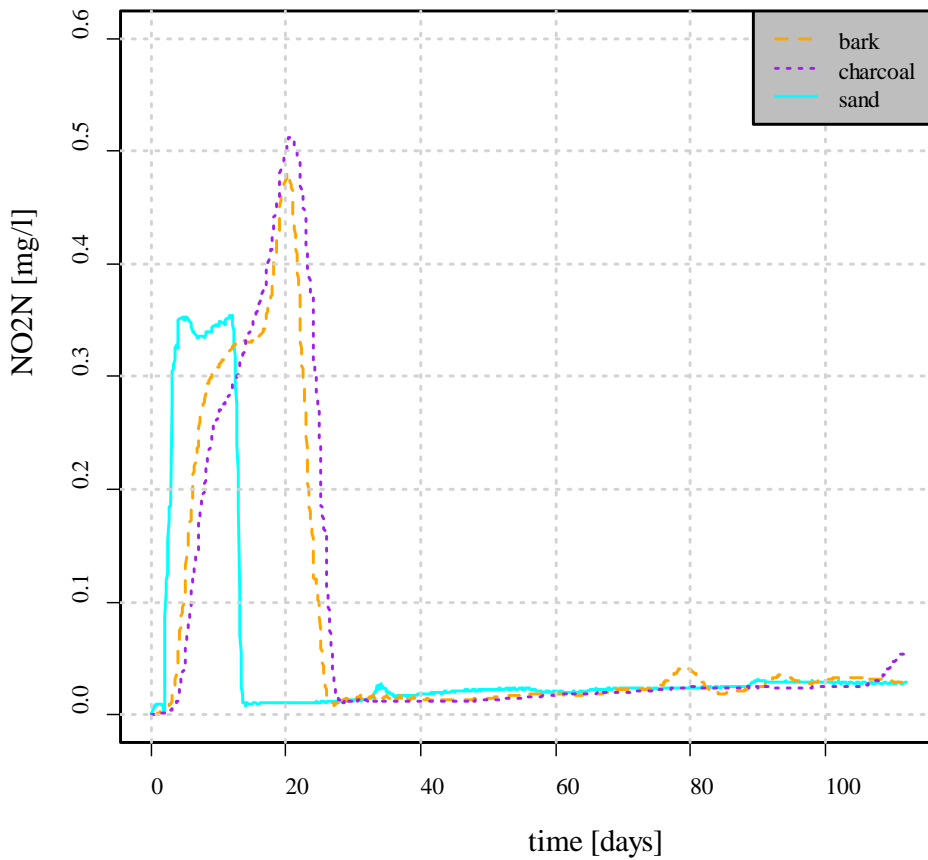


Figure 25 Concentration of nitrite (mg/l) in the filter effluent over time (days) for the bark, charcoal and sand filter.

5.4.4 Dinitrogen concentration

It appeared from the simulations that nitrogen was present throughout the filters. The filters had the largest nitrogen concentration at the immediate top layer of the filter (33 mg/l for bark and charcoal filter, 45 mg/l for sand filter) (Figure 26). In the simulation, nitrogen concentration in the sand filter fluctuated between 19 and 27 mg/l in the top 40 cm of the filter. At filter depth 40-60 cm the nitrogen concentration was constant (22 mg/l) (Figure 26).

The bark and charcoal filters displayed less variation in the nitrogen concentration throughout the filter depth (Figure 26). The bark appeared to contain 18 mg/l nitrogen at depth 10-60 cm and the charcoal filter displayed 21 mg/l nitrogen at depth 20-60 cm (Figure 26).

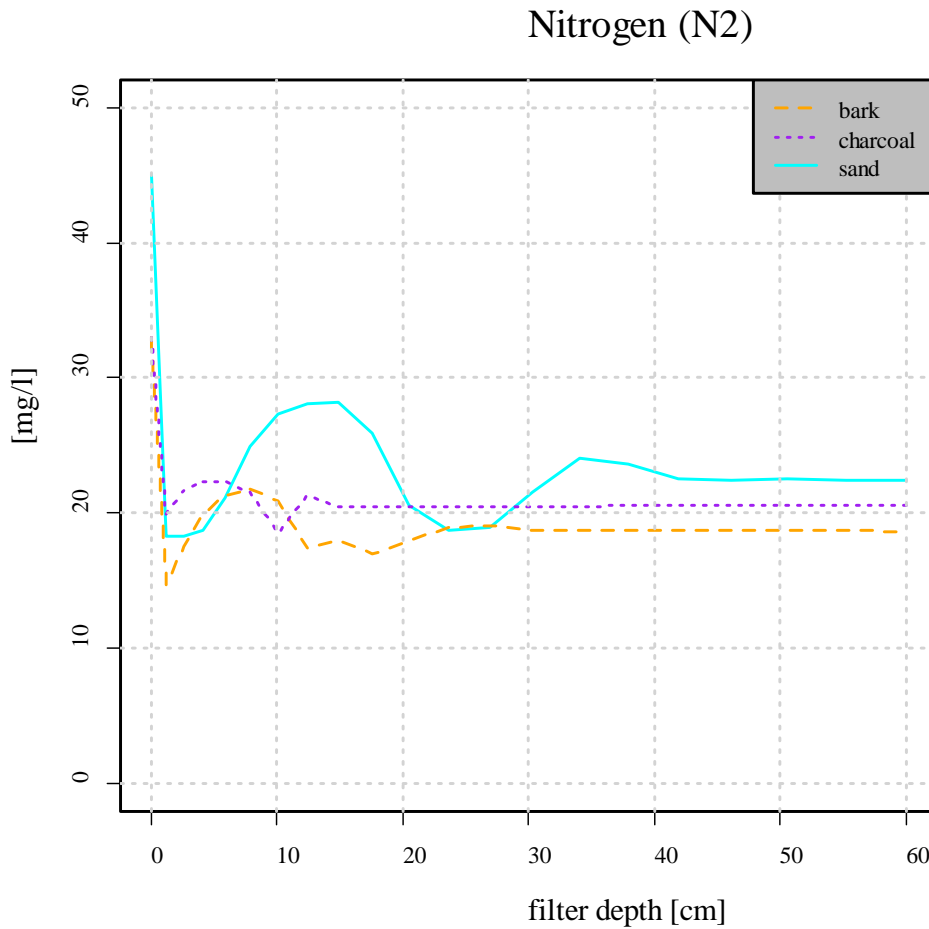


Figure 26 Concentration of nitrogen (mg/l) over filter depth (cm) for the bark, charcoal and sand filter during the last day of simulation (day 113).

5.5 SUMMARIZED RESULTS FOR THE REACTIVE TRANSPORT MODELING

Measurements of effluent concentrations that were available from the precedent experiment were considered to have been measured at steady state. Mean values of the simulated effluent concentrations were taken from the second half of the simulation time span (day 56-113) and were compared to the measured values (Table 8). CR, CS and CI were calculated according to equations 10-12. COD was also included in Table 8 and 9 as CR+CS+CI to demonstrate a value for total organic matter concentration.

Table 8 Simulated and measured mean values of the filter effluent characteristics (day 56-113)

Parameter	Bark		Charcoal		Sand		Inflow [mg/l]
	sim. [mg/l]	meas. [mg/l]	sim. [mg/l]	meas. [mg/l]	sim. [mg/l]	meas. [mg/l]	
CR	0.22	10	0.22	14	0.23	108	425
CS	0.006	4	0.0008	6	0.008	46	180
CI	306	186	308	28	308	91	278
COD	306	200	308	48	308	245	885
IP	0.25	0.06	0.38	0.03	0.45	0.36	2.07
TP	0.98	0.1	1.12	0.3	1.19	0.9	4.2
NO3N	49	51	50	0.15	47	57	1
NH4N	0.098	0.05	0.086	0.07	0.098	3.75	0.46
NO2N*	0.026	-	0.024	-	0.025	-	-
TN**	-	63.85	-	1.3	-	72.2	75.45

* NO2N was not measured

**simulated TN could not be established within the model

Using the values of Table 8, efficient % reduction (%red) was calculated for each parameter with available data by using:

$$\%red = \frac{c_{in} - c_{out}}{c_{in}} \times 100 \quad (13)$$

Where c_{in} is the influent concentration and c_{out} is the filter effluent concentration. The calculated values of %red are displayed in Table 9.

Table 9 Simulated and measured values of efficient reduction (%red), day 56-113

Parameter	Bark		Charcoal		Sand	
	sim.%red [%]	meas.%red [%]	sim.%red [%]	meas.%red [%]	sim.%red [%]	meas.%red [%]
CR	99.9	98	99.9	97	99.9	75
CS	100	98	100	97	100	74
CI*	-	33	-	90	-	67
COD	65	77	65	95	65	72
IP	88	97	82	98.6	78	83
TP	77	98	73	93	72	79
NH4N	79	89	81	85	79	-
TN**	-	15	-	98	-	4

*simulated CI concentration exceeded the influent concentration

**simulated TN could not be established

6. DISCUSSION

6.1 FLOW DYNAMICS

An unexpected occurrence in the empirical experiment was that less water than loaded into the filter emerged as effluent. The loss was larger than what could be expected as loss due to evaporation. This was investigated by looking for leaks and carefully examine the sprinklers, but no leaks were found and the sprinklers distributed an amount with very small deviation (Table 2). Instead it was suspected that air entered the filter and circulated during the night, when no loadings were scheduled. This aeration together with the large specific area of the filter materials resulted in large evaporation losses. When the first loading in the morning occurred, a quite large amount of that water would remain inside the filter to wet the dried out pores instead of emerging as effluent. It appeared in the graphs that mainly water from the first loading was missing, supporting this line of thought (Figures 5-10). If the filters had been more thoroughly covered, the drying out of the filters during the night could have been avoided. Whether it is desirable or not with the air circulation is dependent on the circumstances. Aeration would favor autotrophic bacteria and hence the nitrification process, also the filters would produce less amount of effluent water. If the effluent water is to be used for irrigation and water is scarce, it would not be desirable to loose water due to evaporation.

The overall experiment of simulating the flow dynamics was considered successful since it appeared in the graphs that the simulated data was matching the ones measured (Figures 13-15). There was a slight problem with the flow; the simulated flow was not fast enough after the first daily loading to match the measured. The empirical coefficients, no matter how they were varied, could not adjust the result (Figure 12). When loading occurred, the water from the sprinkler was splashed on the column wall, even when the sprinkler head was adjusted to minimize this. The water may, moreover, run along the column wall, which could explain the fast flow. This could be counteracted by coating the column wall with a soft rubber sheet, which would prevent the large spaces between filter material and the column wall.

It was demonstrated that calibration of empirical coefficients was necessary to obtain a simulated curve with proper fit to the measured data. When the model was run with default values for the empirical coefficients, a good match was not obtained compared to the result of the simulation with calibration (Figures 13-15). This indicated that when setting up a flow model, measured data from an empirical experiment is crucial to develop realistic simulations. Also, though not included in this master thesis, study of retention curves for the filter materials could provide insight on which empirical coefficients to use.

The validation of the empirical coefficients indicated that the chosen values for l , n and α were valid not only for the set of data for which they were designed. They produced a simulation result which also well fitted the measured data for increased flow (Figure 16). The successful validation brought to mind whether it is possible that the chosen

coefficients could be suitable for other circumstances as well. The main target of interest being increased filter area; could the model suffice when scaling up to represent a filter large enough to fit household needs? To answer this, the experiment set-up should be extended to include a filter of larger size so that measured data from it could be used for validation.

6.2 MODELING OF BIOMASS

The simulations demonstrated constant growth of HE in the filters. However, it appeared from the measurements on the physical filters that the concentrations in the effluent did not change with time which indicated that the physical filters were in fact working under pseudo steady state conditions. Hence a pseudo steady state should have been observed in the simulations as well if the model described the filters correctly. It is possible that the parameters concerning microorganism growth should be modified to achieve an earlier pseudo steady state of HE concentration in the simulated filters.

A preceding modeling project had results for surface biomass concentration ranging between 0-30 mgCOD/g DW for sand filters (Leverenz et al., 2008). The highest values of HE concentration in the bark and charcoal filters reached 110 mgCOD/g DW and 200 mgCOD/g DW, respectively. Compared to the range 0-30 mgCOD/g DW these are very high values. The highest concentration of HE in the sand filter (20 mgCOD/g DW) was within the range 0-30 mgCOD/g and hence the results from the sand model appeared as more reasonable than the bark and charcoal model results. Further simulation with an increased time span needs to be done to establish whether the sand filter also would have displayed continued growth of HE to unreasonable extent or if a pseudo steady state would have established with time. From this it would have been possible to conclude whether there was a general error in the model affecting all filters or if something particular was wrong with the bark and charcoal characteristics.

6.3 MODELING OF ORGANIC MATTER DEGRADATION

The simulated organic matter degradation appeared to be similar for all three filters. A significant amount of CR was not present in any filter at any filter depth, most likely because it was immediately incorporated into biomass and used by microorganisms as substrate. It was then transformed into CS, which by hydrolysis could be transformed back into CR. A fraction was transformed into CI due to the decay process of microorganisms. As with the case of CR, CS did not reach a concentration far from zero in any filter at any filter depth.

The concentration of organic matter was instead present in the filter as CI. It could be suspected that the large amount of biomass ensured that organic matter in the form of CR and CS was used up completely by microorganisms and only CI remained as residue.

When the organic matter results of the simulation was compared to measured data, it appeared that simulated and measured values of CR, CS and CI did not compare well for the sand filter (Table 8). If CR, CS and CI were considered together as COD, the results compared quite well with a simulated COD of 308 mg/l and a measured COD of

245 mg/l. This corresponded to a reduction of 65 % and 72 % respectively (Table 9). Consequently, the model could estimate the COD concentration of the sand filter effluent but was not able to describe the constitution of the COD as CR, CS and CI. The reason for the discrepancy could be that the assumptions behind the equations 10-12 do not hold and the influent COD should be divided into CR, CS and CI according to another method.

Since the simulation of CR, CS and CI failed to correspond to the measured values for the sand filter, the results for the bark and charcoal filter needs special caution when looked at. The bark and charcoal displayed low measured concentrations for CR and CS, which coincided well with the simulated results where CR and CS concentrations were close to zero. Simulated results corresponded very well to measured results especially for the efficient % reduction (Table 9). However, for the bark filter, simulated concentration of CI (306 mg/l) did not appear close to the measured CI concentration (186 mg/l). As for the charcoal filter, the simulated concentration of CI (308 mg/l) was not at all comparable to the measured CI concentration (48 mg/l).

The results indicated that the model needed further customizing: adjusting the flow model separately for each filter media was not enough. A reactive transport model that could properly simulate the different characteristics of bark and charcoal compared to sand as filter material was not achieved. From Tables 8-9 it appeared from the measurements on the physical filters that the bark filter had a smaller measured concentration of COD in the effluent (200 mg/l) compared to the sand filter (245 mg/l). The charcoal filter demonstrated an even larger difference, with a measured concentration of COD in the effluent of only 48 mg/l. The different filters when simulated demonstrated very similar concentrations of CR, CS and CI (Figures 17-19). The only distinguishable difference was that the sand filter demonstrated a faster response at start up (Figures 17 and 18).

It is possible that further adjustment of the model, for example tuning adsorption parameters for the charcoal filter material, would be an appropriate approach to further tune the model. When HYDRUS/CW2D was previously used in research for modeling of organic matter degradation in constructed wetlands for treatment of combined sewer overflow, values for parameters describing adsorption for COD was identified by using sensitivity analysis (Henrichs et al., 2007).

For all three filter materials the concentration of inert organic material did not vary with depth (Figure 19). For dimensioning the filter, this indicates that a shorter filter would have a similar effluent.

6.4 MODELING OF NUTRIENT TRANSFORMATION

6.4.1 Phosphorus

According to the simulations, a strong growth of HE (Figure 16) as a result of large amounts of CR available as substrate, formed a large biomass inside the filters. The biomass was mainly formed in the top half of the filters. When the decay of

microorganisms occurred it was expected to release IP, hence concentrations of IP increased in filter depth 20-60 cm.

The simulated concentration of IP in the sand filter effluent (0.45 mg/l) corresponded well to the measured concentration (0.36 mg/l). The simulated TP concentration in the effluent (1.19 mg/l) also compared well to the measured value (0.9 mg/l). However, the simulated results for IP and TP concentrations in the effluent did not compare well to measured values for the bark and charcoal filters. It is possible that the bark and charcoal media holds adsorption properties due to their large specific areas and for this reason prevented phosphorus from desorbing into the effluent. By taking adsorption into account in the model, a better match of simulated and measured values could potentially be achieved for these materials.

It appeared that increasing filter depth would not have decreased the concentration of phosphorus in the effluent, since phosphorus concentration did not decrease with depth (Figure 21).

6.4.2 Nitrogen

It appeared as N₂ was produced in all three simulated filters (Figure 26), indicating ongoing denitrification process by heterotrophic microorganisms. However, the much larger concentration of HE in the bark and charcoal filters compared to the sand filter did not appear to create a difference in the amount of N₂ produced (Figure 26). Nitrogen is produced specifically by NO₃N/NO₂N growth of HE according to the main principles of CW2D. The equality between the filters could be explained by that the NO₃N/NO₂N growth of HE was equal for all three filters. The larger amount of HE in bark and charcoal filter than in sand filter was instead resulting from aerobic growth.

By producing dinitrogen the total nitrogen in the filters should have decreased, since dinitrogen is lost from the filter as gas. This disagrees with measured values of TN in the sand filter effluent (Table 8), as it appears that TN in the effluent (72.2 mg/l) was approximately the same as the influent concentration (75.45 mg/l). A small reduction in TN concentration took place in the bark filter (15 %). Charcoal on the other hand displayed an almost total reduction of TN (98 %). The simulated result for N₂ disagrees with the measured observations.

The simulated sand filter demonstrated an effluent concentration of NO₃N (47 mg/l) that compared quite well to the measured value (57 mg/l). The simulated bark filter appeared to have an effluent concentration of NO₃N (47 mg/l) which was very close to the measured value (51 mg/l). The charcoal filter appeared to be very different from the bark and sand filters with an outgoing concentration of NO₃N near zero (0.15 mg/l). This difference could not be seen in the simulation, where the outgoing concentration of NO₃N was nearly equal for all three filters.

As for the other components simulated with CW2D, it is likely that the model needs further adjustment than the calibration of the hydraulics. The physical charcoal filter

demonstrated near 100 % reduction of total nitrogen which was not simulated by the model.

The NO₃N concentration varied in the filters for filter depth 0-40 but was constant for filter depth 40-60 cm, which indicates that an increased filter depth would not have decreased the concentration of NO₃N in the effluent for any filter (Figure 23).

6.5 MODELING AS A TOOL TO EVALUATE DESIGN CRITERIA

It appears from the simulation that the top 10 cm of the filter is most active in microbial growth (Figure 16) and most of the concentrations are not varying below 40 cm depth (Figures 19, 21, 23, 26). For dimensioning criteria, this indicates that the filter could be shortened without affecting the treatment performance. A shorter filter would be beneficial because of lower production costs and less space required. The treatment capability of the top layer appears from the simulations as very potent. It is natural that the top layer has the most intense activity since it is the place where the easiest degradable substances of the greywater are first received. However, the air-soil boundary might also be of importance to enhance microbial growth and indirectly the treatment performance. If this is the case, a rethinking of filter design might be in order. The vertical filter could be divided into two 30 cm storeys with air in between and free drainage from the first part down to the second part. It would be similar to having vertical filters in parallel, but shorter and stacked on top of each other.

Regarding shorter vertical filter depth, design guidelines are usually only declaring the required area per personal equivalent (pe). For example in Denmark, the necessary surface area of the filter bed is 3.2 m²/pe and the effective filter depth is 1.0 (Brix, 2005). Further research on how filter depth of vertical flow filters affects treatment performance could provide important conclusions for developing design criteria.

6.6 RECENT RESEARCH ASSOCIATED TO CW2D

The CW2D module is a fairly new component of HYDRUS and is still in need of further validation. The greatest issue of concern is how to empirically measure the module parameters, especially in regard to the reactive transport. Determining the parameters by measurements is crucial to calibrating the model.

Measurement of microbial biomass in an indoor pilot-scale CW provided insight on the model parameters concerning the microorganisms (Langergraber, et al., 2007). With some calculation the measurements of microbial biomass were converted to the theoretical biomass COD which is simulated by CW2D. The calculated conversion made it possible to compare measured and simulated biomass.

To gain a better fit between measured and simulated biomass, heterotrophic lysis rate constants were chosen for modification (Langergraber, et al., 2007). However, the simulated data could not be wholly adjusted to measured data by only adjusting the heterotrophic lysis rate constants. The biomass COD seemed to be over predicted in the 1-5 cm depth and under predicted in the 5-10 cm depth. It might be that the influence of biomass growth on the hydraulic properties has to be included into the model in order to

correct this, but this is not yet possible to achieve within the HYDRUS/CW2D software package (Langergraber, et al., 2007).

Another step towards calibration of CW2D was made by investigating the treatment performance of outdoor subsurface flow CW (Langergraber, 2005). The main target was to study the models performance in regards to the varying temperature of a temperate climate. Three subsurface vertical flow beds with surface area of about 20 m² each were built in Ernsthofen (Lower Austria). Sandy substrate of gravel size 0.006-4 mm was used as main filter material. The flow beds were loaded with hydraulic loading rate 32.2, 43.0 and 64.7 mm/day and organic loading rate 20, 27 and 40 g COD /m²day during 20 months, including two winters. The temperature varied between 4 and 18 °C. Effluent concentrations of COD, BOD₅, NH₄N and NO₃N were measured and compared to simulated data.

For the low temperatures, the model was not able to simulate data with a good fit to measured data when using the standard parameters (Langergraber, 2005). To adjust the model, temperature dependencies for half-saturation constants for the hydrolysis and nitrification processes were introduced. Something similar to this was done previously for a set of parameters in ASM1 and when applied in CW2D, the simulation results matched measured data well. However, this new parameter set should be tested on other CW systems for validation before it is put to practical use (Langergraber, 2005).

6.7 GENERAL REMARKS

The simulated growth of microorganisms appeared for all filters to be most intense in the top layer of the filters, indicating that the top part of the filter will be central to the processes connected to the microorganisms.

The simulations indicated there might be larger concentrations of NO₂N, NO₃N and CR emerging in the filter effluent during startup of the filter (Figures 17, 24, 25). However, this was not recorded in the measurements of the physical filters. The underlying assumption for the models that the filters were clean at startup (zero concentration as initial condition) might have caused an erroneous behavior initially.

The simulated concentrations of Cl, NO₃N and N₂ appeared to be considerably larger at the surface of the filter than in any depth (Figures 19, 23, 26). When evaporation was excluded from the model, the filter surface did not display high concentrations, indicating that evaporation of the surface was the cause of the discrepancy.

It appeared from the simulations that the simulated behavior of the three filter types in fact did not produce different results, even though the measured data indicated quite large differences between the filters.

There was reason to question the suitability of using CW2D for modeling bark and charcoal filters. CW2D is meant for modeling of constructed wetlands, which uses natural soils as filter media. Although the sand filter was equal to a natural soil filter and the charcoal had a similar build to gravel, the bark was subject to significant swelling

when wetted. Swelling affects the filter behavior and is not possible to model with neither HYDRUS nor CW2D. Also, both charcoal and bark could be suspected to have properties related to their large specific area, such as enhanced adsorption qualities. There are adsorption parameters in HYDRUS but they were not changed from the default values when modeling the bark and charcoal filter. It is possible that if these adsorption parameters were to be adjusted according to the properties of bark and charcoal, the model would be able to catch the differences between the materials.

The sand filter model might need adjustment of parameters concerning HE growth and decay. The continuous growth of HE was not expected to proceed throughout the simulation time span. In spite of this, the simulated sand filter results proved to match the measured data quite well.

The simulation results strongly indicated that adjusting the hydraulic properties was not enough to simulate the expected reactive transport results for bark and charcoal filters. The excessive amount of parameters available for tuning the model further is both good and bad. A user cannot easily orientate through the parameter set and to decide what to adjust becomes overwhelming. With time and skill on the other hand, a user has the possibility to produce models that includes great amounts of detail and hopefully along with detail also accuracy in the results.

7. REFERENCES

- Aktar, W., 2007. Sewage water pollution and its environmental effects. *Free Online Articles Directory*. Published online: 26 May 2007
- Brix, H., Arias, C., 2005. The use of vertical flow constructed wetlands for on-site treatment of domestic wastewater: New Danish guidelines. *Ecological Engineering*, Volume 25 p. 491-500
- Dalahmeh, S., Pell, M., Vinnerås, B., Hylander, L., Öborn, I., Jönsson, H., 2012. Efficiency of Bark, Activated Charcoal, Foam and Sand Filters in Reducing Pollutants from Greywater. *Water Air Soil Pollut.* Published online: 29 March 2012
- Eriksson, J., Nilsson, I., Simonsson, M., 2005. *Wiklanders MARKLÄRA*. Lund: Studentlitteratur
- Haberl, R., Grego, S., Langergraber, G., Kadlec, R., Cicalini, A., Dias, S., Novais, J., Aubert, S., Gerth, A., Thomas, H., 2003. Constructed Wetlands for the Treatment of Organic Pollutants. *Journal of Soils and Sediments*, Volume 3 (2) p. 109-124
- Henrichs, M., Langergraber, G., Uhl, M., 2007. Modeling of organic matter degradation in constructed wetlands for treatment of combined sewer overflow. *Science of the Total Environment*, Volume 380, p. 196-209
- Henze, M., Grady, L., Gujer, W., Marais, G., Matsuo, T., Wentzel, M., Loosdrecht, M., Mino, T., 2002. Activated Sludge Models ASM1, ASM2, ASM2D and ASM3. *Scientific and Technical Report No 9, IWA Publishing*. Available at: <<http://scholar.google.se/>> [Accessed 2012-08-06]
- Langergraber, G. and Muellegger, E., 2004. Ecological Sanitation – a way to solve global sanitation problems? *Environment International*, Volume 31, p. 433-444
- Langergraber, G., 2005. Simulation of the treatment performance of outdoor subsurface flow constructed wetlands in temperate climates. *Science of the Total Environment*, Volume 380, p. 210-219
- Langergraber, G. and Simunek, J., 2005. Modeling Variably Saturated Water Flow and Multicomponent Reactive Transport in Constructed Wetlands, *Vadose Zone Journal*, Volume 4, p.924-938
- Langergraber, G., 2007. Modeling of Processes in Subsurface Flow Constructed Wetlands: A Review. *Vadose Zone Journal*, Volume 7 (2) p. 830-842
- Langergraber, G., Tietz, A., Haberl, R., 2007. Comparison of measured and simulated distribution of microbial biomass in subsurface vertical flow constructed wetlands. *Water Science & Technology*, Volume 56 (3) p. 233-240

Langergraber, G. et al., 2008. Recent developments in numerical modeling of subsurface flow constructed wetlands. *Science of the total environment*, Volume 407 p. 3931-3943.

Langergraber, G., 2011. Numerical modeling: a tool for better constructed wetland design? *Water Science & Technology*, Volume 64 (1), p. 14-21

Leverenz, H., Tchobanoglous, G., Darby, J., 2008. Clogging in intermittently dosed sand filters used for wastewater treatment. *Water research*, Volume 43 p. 695-705

Muellegger, E., Langergraber, G., Jung, H., Starkl, M., Laber., J., 2003. Potentials for greywater treatment and reuse in rural areas. *Ecosan-closing the loop – Proceedings of the 2nd International Symposium on ecological sanitation*, p. 799-802. Available through: Ecosan Club website <<http://www.ecosan.at/info/workshops/potentials-for-greywater-treatment-and-reuse-in-rural-areas.pdf>> [Accessed 2012-03-19]

Ottoson, J., 2005. *Comparative analysis of pathogen occurrence in wastewater*. Doctoral Thesis. Stockholm: Royal Institute of Technology.

Simunek, J. and van Genuchten, M.Th. and Sejna, M., 2006. The HYDRUS Software Package for Simulating the Two- and Three-Dimensional Movement of Water, Heat and Multiple Solutes in Variably-Saturated Media Technical Manual Version 1.0, *PC-Progress Engineering software developer*. Available at: <http://www.pc-progress.com/Downloads/Pgm_Hydrus3D/HYDRUS3D%20Technical%20Manual.pdf> [Accessed 2012-03-22]